Identifying Novel Interaction Between the E3 Ubiquitin Ligase Ring Finger Protein 20 (RNF20) and the Deubiquitinating Enzyme Ubiquitin Specific Protease 7 (USP7)

A THESIS SUBMITTED TO THE FACULTY OF GRADUATE STUDIES IN

PARTIAL FULFILLMENT OF THE REQUIREMENTS FOR THE DEGREE OF

MASTER OF SCIENCE

GRADUATE PROGRAM IN BIOLOGY

YORK UNIVERSITY

TORONTO, ONTARIO

November 2025

Abstract

USP7, which is a ubiquitin-specific protease, is an essential deubiquitinating enzyme involved in a plethora of cellular processes such as epigenetic regulation, DNA damage response and oncogenic processes. In this study, RNF20, which is an E3 ligase, has been identified as a novel substrate for USP7. Through various biochemical and functional assays, including endogenous co-immunoprecipitation, comparing parental and USP7 knockout HCT116 cells, reconstitution assay, overexpression with USP7 or the catalytic mutant USP7, cycloheximide chase and a deubiquitination assay, we show that RNF20 stability is dependent upon USP7 removing ubiquitin chains that would mark RNF20 for proteasomal degradation. This interaction was seen within multiple cell lines, with the catalytic activity of USP7 being crucial to the stability of RNF20. These findings provide the foundation for future studies on how the regulation of RNF20 through USP7 can contribute to epigenetic regulation, DNA damage response, and oncogenic processes.

Acknowledgments

First and foremost, I would like to thank and acknowledge my supervisor, Dr. Vivian Saridakis, for granting me this opportunity to join her lab. I am incredibly grateful for the endless support, guidance and patience she has shown me during my journey. Her mentorship not only helped me complete this thesis but also greatly influenced me to grow as a scientist.

I would also like to sincerely thank Dr. Bayfield for being a part of my supervisory committee and taking the time to review and revise my work. His insightful critiques and suggestions greatly helped in shaping the direction of my project.

Thank you to my fellow lab members, Kanwar, Serena and Sukhdeep, for constantly being there when I needed help with anything in the lab and for training me in the various techniques I used throughout my project. I would also like to thank all the friends I made in LSB and around campus for all the laughs and good times spent on campus.

Lastly, I cannot forget to thank my family for their endless support during this process. Without their support, help and encouragement, this research would not have been possible.

Table of Contents

List of Figures

List of Abbreviations

ABRO1	Abraxas Brother 1
AMSH	Associated Molecule with the SH3 domain of STAM
ATM	Ataxia-Telangiectasia Mutated
ATP	Adenosine triphosphate
ATXN	Ataxin
BAP1	BRCA1 Associated Protein 1
BLM	Bloom Syndrome Protein
BMI1	B cell-specific Moloney murine leukemia virus integration site 1
BRCC36	BRCA1/BRCA2-containing complex subunit 36
CDK8	Cyclin-Dependent Kinase 8
Chk	Checkpoint Kinase
Co-IP	co-Immunoprecipitation
CSN5	COP9 signalosome complex subunit 5
CSN6	COP9 signalosome complex subunit 6
CTD	C-Terminal Domain
DDR	DNA Damage Response
DNMT1	DNA Methyl Transferase 1
DSB	Double-Strand Break
DUB	Deubiquitinating Enzyme
E1	Ubiquitin Activating Enzyme
E2	Ubiquitin Conjugating Enzyme

E3	Ubiquitin Ligase
EBNA1	Epstein–Barr Nuclear Antigen 1
EBV	Epstein-Barr Virus
ELF3H	Eukaryotic Translation Initiation Factor 3 Subunit H
ELF3F	Eukaryotic Translation Initiation Factor 3 Subunit F
EZH2	Enhancer of Zeste Homolog 2
FOXO1	Forkhead box O Protein 1
HAT	Histone Acetyltransferase
HAUSP	Herpesvirus Associated Ubiquitin Specific Protease
HCT116	Human Colorectal Carcinoma Cell Line
HDAC	Histone Deacetylases
HECT	Homologous to E6AP C-Terminus
HEK293T	Human Embryonic Kidney 293T
HR	Homologous Recombination
HSV-1	Herpes Simplex Virus Yype 1
ICN1	Intracellular NOTCH1
JAMM	JAMM Motif Proteases
KSHV	Kaposi’s Sarcoma-associated Herpesvirus
KU70	Ku Protein Subunit 70
Lys	Lysine
MATH	Meprin and TRAF Homology
MCF7	Michigan Cancer Foundation-7

MDC1	Mediator of DNA Damage Checkpoint 1
MDM2	Mouse double minute 2 homolog
MJD	Josephin Domain Proteases
MPN	Mpr1–Pad1 N-terminal domain
MYSM1	Myb-like, SWIRM, and MPN-domain–containing protein 1
NHEJ	Non-Homologous End Joining
OTU	Ovarian Tumour Proteases
OTUB1	OTU domain-containing ubiquitin aldehyde-binding protein 1.
PAGE	Polyacrylamide Gel Electrophoresis
PBS	Phosphate Buffered Saline
PPM1G	Protein Phosphatase 1G
PHF8	PHD Finger Protein 8
PRC	Polycomb Repressive Complex
RBR	RING-between-RING
RING	Really Interesting New Gene
RNF	Ring Finger Protein
Rpn	Regulatory Particle Non-ATPase
Rpt	Regulatory Particle ATPase
RPS27A	ribosomal protein S27a
SDS	Sodium Dodecyl Sulfate
SIRT7	Sirtuin 7
SMURF2	SMAD Specific E3 Ubiquitin Protein Ligase 2

T-ALL	T-cell Acute Lymphoblastic Leukemia
TBS	Tris-buffered Saline
TIP60	Tat-Interactive Protein 60
TNF	Tumour Necrosis Factor
TRABID	TRAF-binding domain-containing protein
TRAF	Tumor Necrosis Factor Receptor–Associated Factor
UBA1	ubiquitin-like modifier activating enzyme 1
UBA6	ubiquitin-like modifier-activating enzyme 6
UBA52	Ubiquitin A-52 Residue Ribosomal Protein Fusion Gene
UBB	Ubiquitin B Gene
UBC	Ubiquitin C Gene
UBL	Ubiquitin Like
UCH	ubiquitin C-terminal hydrolases
UHRF1	Ubiquitin-like with PHD And Ring Finger Domains
UIM	ubiquitin interaction motif
USP	Ubiquitin Specific Proteases
USP7	Ubiquitin Specific Protease 7
vIRF1	Viral Interferon Regulatory Factor 1
Vmw110	Virus-encoded Molecular Weight 110 kDa

CHAPTER 1: INTRODUCTION

1.1 Ubiquitination in Cellular Protein Regulation

There are thousands of proteins found within living systems, each with its unique role in maintaining homeostasis within the organism. These proteins are constantly being synthesized, modified, and degraded as part of the cell's ongoing processes. These processes require intricate checks and regulation, which are crucial to the cell's normal function, growth and viability. One of these regulatory systems utilizes the addition and removal of ubiquitin to modulate the activity, localization or turnover of target proteins. The addition of these ubiquitin chains (polyubiquitin chains) can mark proteins for degradation via the 26S proteasome. Proteins may be targeted for degradation for numerous reasons, including misfolding after synthesis, which can alter their function. If these defective proteins are not removed, it may lead to harmful outcomes such as cancerous growths and disease. In contrast, monoubiquitination tags can modulate protein activity and localization, depending on where the ubiquitin tags are added.

1.2 Ubiquitin

Ubiquitin is a highly conserved 76-amino-acid-long protein (8.5 kDa) which can be added and removed from various residues on target substrates (Weissman, 2001). Ubiquitin is derived from 4 distinct genes within humans, which are *UBB, UBC, UBA52* and *RPS27A*. Two of these genes, *UBA52* and *RPS27A,* produce ribosomal fusion proteins where the ribosome is fused to a single ubiquitin. Whereas the other two genes, *UBB* and *UBC*, encode polyubiquitin precursors, which consist of three and nine head-to-tail ubiquitin repeats. Deubiquitinating enzymes (DUBs)

can then cleave those ubiquitin repeats, releasing free ubiquitin, which can be used in various cellular processes (Heride et al., 2014). To support the wide range of functional outcomes associated with ubiquitination, ubiquitin can be attached to target proteins in three distinct forms: monoubiquitination, multi-monoubiquitination, and polyubiquitination (Figure 1). Monoubiquitination involves the addition of a single ubiquitin to the target substrate, which can lead to downstream effects such as increased protein stability and acting as a signal for proteins to enter the nucleus (Yang et al., 2017). Multi-monoubiquitination is the addition of multiple single ubiquitin molecules to many sites on a substrate, which can play a role in the substrate localization (Haglund et al., 2003). Polyubiquitination represents another critical form of ubiquitination, in which ubiquitin molecules are linked together in either linear or branched chain configurations (Figure 1). In linear (homotypic) chains, each ubiquitin is attached to the same lysine residue as the preceding ubiquitin, resulting in a uniform linkage. In contrast, branched chains involve the attachment of additional ubiquitin to different lysine residues, creating a more complex and heterogeneous structure. Each ubiquitin molecule contains seven distinct lysine residues, Lys6, Lys11, Lys27, Lys29, Lys33, Lys48 and Lys63, to which additional ubiquitin may be added to create the linear or branched ubiquitin chains (Ziv et al., 2011).

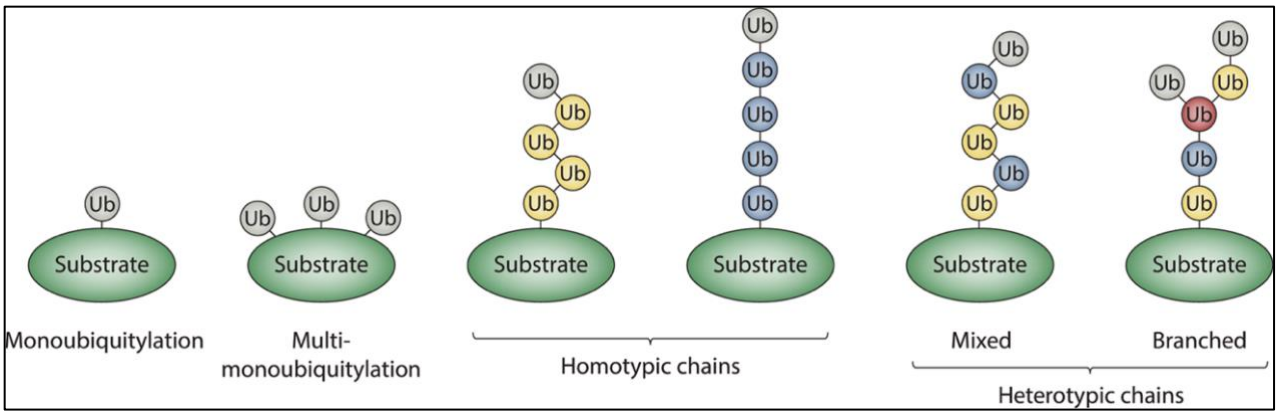

Figure 1. Classification of ubiquitin modifications.
Illustration of the addition of ubiquitin molecules to substrates in various ways, including monoubiquitination, multi-monoubiquitination, and polyubiquitination, which can be further subdivided into homotypic (linear) or heterotypic (branched) chains. The various colours indicate how each ubiquitin is modified/linked with blue or yellow, showing ubiquitin linked through a single acceptor site, red indicating the branching point and grey displaying the terminal ubiquitin. Adapted from French, Koehler, and Hunter (2021).

1.3 Ubiquitination

The addition of ubiquitin, known as ubiquitination, is a post-translational modification that affects the stability, activity, and localization of the protein to which it is attached (Zhou et al., 2021a). The process of ubiquitination occurs via three enzymes: first is E1, the ubiquitin activation enzyme, followed by E2, which is a ubiquitin-conjugating enzyme and finally E3, the ubiquitin-protein ligase (Pickart & Eddins, 2004). There are two known human E1 enzymes (UBA1 and UBA6), approximately 40 E2 enzymes, and about 600 E3 enzymes. The ubiquitination pathway begins when the E1 enzyme activates ubiquitin in an ATP-dependent manner, forming a high-energy thioester bond between the C-terminal glycine of ubiquitin and a catalytic cysteine residue in the E1 enzyme. This activated ubiquitin is then passed to a cysteine residue on an E2 conjugating enzyme through a thiol–ester exchange reaction, resulting in the formation of an E2-ubiquitin thioester intermediate. In the final stage, the E2-ubiquitin complex interacts with an E3 ligase, which facilitates the transfer of ubiquitin to a lysine residue

on the target protein. The E3 ligase ensures proper positioning of the substrate and E2-ubiquitin, promoting the formation of an isopeptide bond between ubiquitin and the ε-amino group of a lysine on the substrate (Pickart & Eddins, 2004). Successive rounds of ubiquitination result in the formation of polyubiquitin chains, the functional outcome of which is determined by the specific lysine residue through which the ubiquitin molecules are linked. These distinct linkage types act as molecular codes that signal different cellular processes (Figure 2). For example, K48-linked chains represent the canonical signal for proteasomal degradation, thereby regulating protein turnover and maintaining protein homeostasis. In contrast, K63-linked chains are primarily involved in non-proteolytic functions, such as activating the NF-κB signalling pathway, which is essential for immune responses, inflammation, and cell survival. Less commonly, K6-linked chains have been associated with the DNA damage response, where they promote the recruitment of DNA repair factors to sites of genomic instability (Musaus et al., 2020). With more than 600 distinct E3 ligases governing the ubiquitylation of thousands of protein substrates, precise regulation of E3 ligase activity is essential to ensure specificity and fidelity in substrate recognition and modification (Buetow & Huang, 2016). Three major classes of E3 ligases have been identified: RING (Really Interesting New Gene), HECT (Homologous to E6AP C-Terminus), and RBR (RING-between-RING). RING-type E3s function as scaffolds, catalyzing the direct transfer of ubiquitin from the E2 conjugating enzyme to the substrate without forming a covalent intermediate. In contrast, HECT E3 ligases operate through a two-step catalytic mechanism: they first receive ubiquitin from the E2 ubiquitin thioester intermediate, which is then transferred to a lysine residue on the target substrate (Buetow & Huang, 2016). Lastly, the RBR E3 ligases use a hybrid method between RING and hect E3 ligases,

where the first ring domain of the RBR E3 ligase binds to the E2, allowing for the transfer of the ubiquitin molecule from the E2 to the second ring domain on the RBR E3 ligase before the ubiquitin is transferred to the target substrate (Cotton & Lechtenberg, 2020.) Overall, ubiquitination serves as a crucial regulatory mechanism that controls protein stability and function, thereby influencing a wide range of cellular processes.

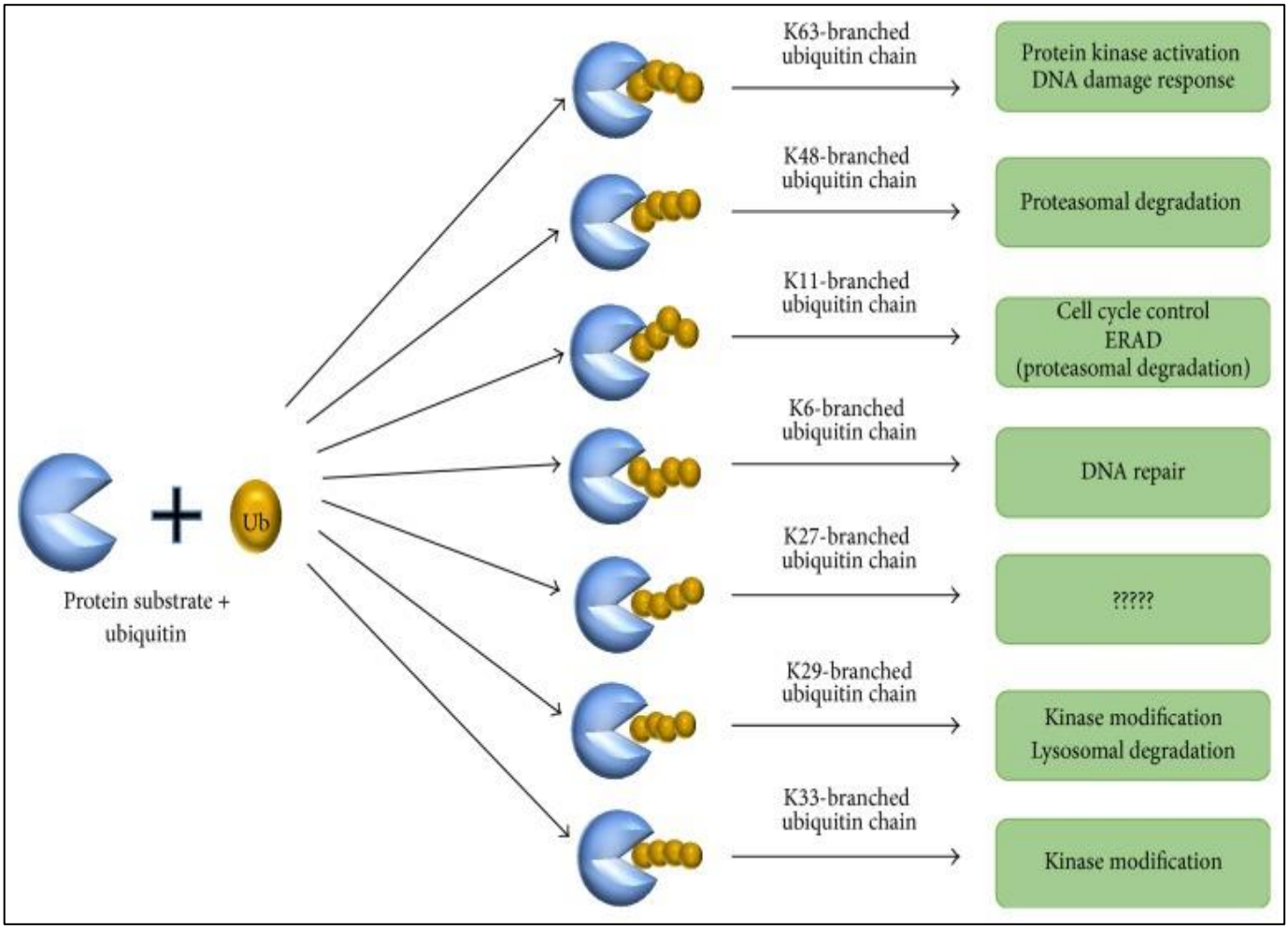

Figure 2. Ubiquitin modifications and their cellular functions.
Downstream pathways of polyubiquitination involve ubiquitin chains linked via lysine residues, regulating diverse cellular functions. Adapted from Suresh, Lee, Kim, and Ramakrishna (2016).

1.4 Deubiquitination

With the addition of ubiquitin being a valuable post-translational modification that can control the fate of a substrate in a plethora of ways, it must be reversible. The process of removing ubiquitin tags from the substrate is known as deubiquitination. The enzymes responsible for deubiquitinating ubiquitinated substrates are called deubiquitinating enzymes or DUBs (J. Liu et al., 2021). DUBs play essential roles in maintaining cellular balance and regulating protein function. They help produce free ubiquitin by processing precursor forms, such as polyubiquitin chains or ubiquitin fused to ribosomal proteins. DUBs also remove ubiquitin from modified proteins, which can either halt signalling processes or prevent proteins from being degraded by the proteasome or lysosome. Even after proteins are marked for degradation, DUBs recover and recycle ubiquitin to support its availability in the cell. Additionally, DUBs fine-tune ubiquitin signalling by trimming or reshaping ubiquitin chains (Komander et al., 2009). The human genome encodes about 100 DUBs, divided into five classes (Sowa et al., 2009). The five main classes of deubiquitinating enzymes include cysteine proteases, ubiquitin-specific proteases (USPs), ovarian tumour proteases (OTUs), ubiquitin C-terminal hydrolases (UCHs), Josephin domain proteases (MJDs), and the Jab1/Mov34/Mpr1 (JAMM) family of metalloproteases (Wolberger, 2014). USPs are the largest DUB family, featuring three subdomains in its structure: the palm, thumb, and finger domains. The catalytic site is located between the palm and thumb domains. In USPs, the catalytic site is a conserved domain of 350 amino acids containing a catalytic triad of three amino acids that are essential to the catalytic activity. The amino acids in the triad are cysteine (C223), histidine (H464), and aspartate (D481), which facilitate cleavage of the isopeptide bond between ubiquitin's C-

terminus and the substrate (Keijzer et al., 2024). The finger domain binds to a distal ubiquitin and stabilizes the complex, enabling USPs to perform their catalytic function. There have been sixteen human OTU Dubs identified, with specificity for certain linkages: OTUB1 is K48-specific, Cezanne is K11-specific, TRABID is K29/K33-specific, and OTULIN is M1-specific (Mevissen et al., 2013). There are 4 UCH DUBs: UCH-L5, UCH-L1, UCH-L3, and BAP1. All four UCH family members share a conserved catalytic region with an α-β-α sandwich fold, which is the canonical structure for UCH DUBs, as well as a crossover loop over the active site that prevents larger substrates from accessing it (Xu, 2024). Currently, four human MJD DUBs have been identified: TXN3/ataxin3, ATXN-3L, JOSD-1, and JOSD-2. All four MJD DUBs contain a highly conserved catalytic triad of two histidines and one cysteine. Additionally, ATXN3 and ATXN3L feature a UIM (ubiquitin interaction motif), thought to stabilize the interaction with ubiquitin (Li & Reverter, 2021). The JAMM family of metalloproteases, unlike cysteine proteases, uses Zn^{2+} ions coordinated by serine, histidine, and aspartate residues to activate a water molecule, enabling deubiquitination (Pan et al., 2022). In humans, 12 JAMM family proteins have been identified, with 7 being catalytically active MPN^{+} members and 5 inactive MPN^{-} members. The MPN^{+} proteins include AMSH, AMSH-LP, BRCC36, ELF3H, Rpn11, CSN5, and MYSM1, while the MPN^{-} group consists of Abraxas, Abro1, CSN6, ELF3F, and Rpn8 (Pan et al., 2022). The MPN (Mpr1-Pad1 N-terminal) domain determines whether the JAMM family protease is catalytically active or inactive: MPN+ proteins are active, containing the zinc-coordinating JAMM motif, while MPN^{-} proteins serve as scaffolds in JAMM multi-subunit complexes (Pan et al., 2022).

1.5 26S-Proteasome Dependent Degradation

The 26S proteasome is the cell's quality control and recycling center of the cell, where 80% of the cell's protein degradation takes place. The 26S proteasome primarily identifies the proteins that have the K48 polyubiquitin tag and degrades them. This process includes both the breakdown of misfolded and improperly assembled proteins, as well as the slower degradation of bulk proteins (Collins & Goldberg, 2017). Once the 26S proteasome has processed the polypeptides marked for degradation, the output is short peptides ranging from two to ten residues in length for 90% of the proteins processed (Kisselev et al., 1999). The 26S proteasome is a multi-catalytic, ATP-dependent protease complex approximately 2.5 MDa in size (Livneh et al., 2016). It is composed of a 20S core particle and two 19S regulatory particles (Figure 3). The 20S core is a hollow cylinder with two outer alpha rings and two inner beta rings forming the proteolytic centre (Smith et al., 2005). Each alpha ring consists of seven alpha subunits forming a narrow channel that regulates substrate entry into the 20S core. Each beta ring contains seven beta subunits, of which only three possess proteolytic active sites situated within the interior of the 20S core (Livneh et al., 2016). The 19S regulatory particle recognizes ubiquitinated substrates, catalyzes the removal of ubiquitin moieties, mediates substrate unfolding, and facilitates their translocation into the 20S core for subsequent proteolytic degradation (Habib et al., 2022). The 19S regulatory particle is made of two subcomplexes: the lid and the base, which include multiple subunits with ubiquitin-binding sites, ATPase catalytic centres, and deubiquitinating enzymes (Rosenzweig et al., 2008). The base functions both as a structural scaffold and a substrate entry gate. It is composed of two leucine-rich proteins, Rpn1 and Rpn2, six ATPase subunits (Rpt1–Rpt6) and non-ATPase subunits such as Rpn13 and Rpn10,

all situated adjacent to the 20S core (Glickman et al., 1998; Tomko & Hochstrasser, 2011). The 19S lid has nine Rpn subunits, Rpn3, Rpn5–Rpn9, Rpn11, Rpn12, and Rpn15, which facilitate the recognition of ubiquitinated substrates and catalyze their deubiquitination, a crucial step before degradation by the 20S core (Habib et al., 2022; Marescal & Cheeseman, 2025).

The process of ubiquitin-dependent degradation via the 26S proteasome begins with substrate recognition by the 19S regulatory particle, which contains ubiquitin recognition sites Rpn1, Rpn10, and Rpn13 (Davis et al., 2020). Once these recognition sites have identified the target protein, ATPases Rpn1-6, through multiple cycles of ATP hydrolysis, mechanically unfold the protein while feeding the unfolded substrate into the 20S core (Davis et al., 2020). During substrate translocation into the 20S core, the essential deubiquitinase Rpn11 catalyzes the *en bloc* removal of polyubiquitin chains. This removal prevents premature deubiquitination, ensuring that the ubiquitin tags remain attached until the substrate reaches the translocation machinery, which reduces the risk of early substrate release (Davis et al., 2020; Matyskiela et al., 2013). Besides Rpn11, accessory deubiquitinases associated with the 19S regulatory particle assist in ubiquitin recycling and can influence degradation efficiency by trimming or editing ubiquitin chains before Rpn11-mediated cleavage. After the substrate has been deubiquitinated and unfolded, the 20S core particle executes its proteolytic function through its β-subunits, which contain the active sites for proteolysis. These catalytic subunits cleave the polypeptide into smaller peptide fragments, completing the degradation process (Navon & Ciechanover, 2009).

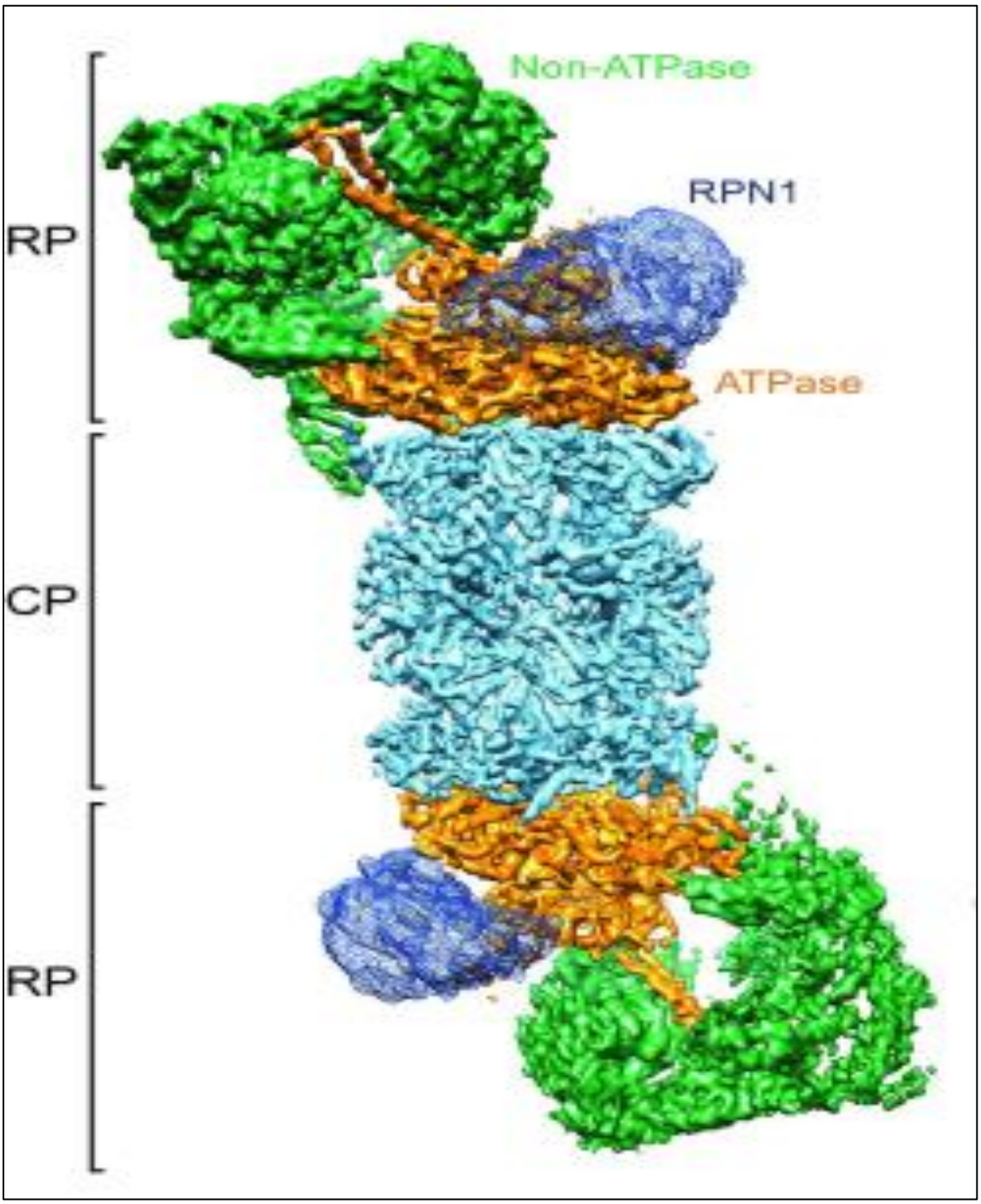

Figure 3. Schematic illustration of the 26S proteosome.
Structure of the 26S proteosome, highlighting the regulatory particle (RP, green) and core particle (CP, blue). Adapted from Mao (2021).

1.6 Ubiquitin Specific Protease 7

USP7, which is a member of the ubiquitin-specific protease family, is known as a deubiquitinating enzyme (DUB). Also referred to as herpesvirus-associated ubiquitin-specific protease (HAUSP), it is a cysteine protease consisting of 1,102 amino acid residues (135 KDa), which has 3 domains: a tumour necrosis factor (TNF) receptor-associated factor (TRAF) like domain at its N-terminus, also known as the Meprin and TRAF Homology (MATH) domain, a catalytic domain, and a C-terminus domain containing ubiquitin-like domains (UBL) (Figure 4)(L. Zhou et al., 2021). USP7 was identified as a novel DUB that is a part of the USP family in 1997 for its novel interaction with the early regulator protein for herpes simplex virus type 1 (HSV-1) Vmw110 (Z. Wang et al., 2019). USP7 was later found to interact with other viral proteins, including EBNA1 from Epstein-Barr virus (EBV) and vIRF1 from Kaposi's sarcoma-associated herpesvirus (KSHV)(Chavoshi et al., 2016; Holowaty et al., 2003). USP7 has since been found to play a role in several critical cellular processes, such as the key signalling pathway Wnt/β-Catenin, which plays a role in embryonic development and tissue homeostasis (Kwon et al., 2013). It has been reported that USP7 is a negative regulator of the pathway due to its interaction with Axin, where it deubiquitinates and stabilizes it, thereby repressing the Wnt/β-Catenin pathway (Ji et al., 2019). Another key signalling pathway is the NOTCH pathway, which plays a role in a plethora of cellular processes such as organ formation and development (Zhou et al., 2022). In particular, NOTCH1 interacts with USP7 and plays a role in T-cell acute lymphoblastic leukemia (T-ALL), where USP7 promotes leukemia growth by stabilizing the levels of NOTCH1 (Jin et al., 2018). USP7 also plays an essential role in epigenetic regulation by modulating the ubiquitination status of histone H2B, thereby influencing gene expression.

Additionally, USP7 contributes to the cellular viral response by regulating p53 ubiquitination (Zhou et al., 2021).

1.7 Structure of USP7

USP7 is comprised of three domains: the N-terminus TRAF/MATH domain, which is involved in recruiting target substrates, the catalytic domain, which carries out the DUB reaction and the C-terminus UBL domain, which has a substrate binding domain (Figure 4) (Kim et al., 2016). The N-terminus TRAF/MATH domain of USP7 is a single domain with a distinctive feature, which is the eight-stranded antiparallel β-sandwich fold which spans residues 53-205 (Saridakis et al., 2005). The TRAF/MATH domain contains the ^{164}DWGF^{167} motif, as shown in Figure 4, which recognizes a P/A/ExxS motif on target substrates, such as the PGGS motif on p53 (Sheng et al., 2006). The P/A/ExxS motif is situated within a shallow groove of the TRAF/MATH domain, where the residues D164 and W165 function as critical anchoring points that facilitate the recognition and binding of consensus sequences in target substrates. Mutation studies were conducted, in which D164 and W165 were individually substituted with alanine, demonstrating that disruption of these anchoring residues abolishes substrate binding by destabilizing the interaction within the TRAF/MATH groove, highlighting their essential contribution to substrate recognition (Sheng et al., 2006).

The catalytic domain of USP7 spanning residues 208-560, like all other USPs, takes on the right-hand configuration where there are the palm, thumb and finger protein domains. The region between the palm and thumb is where the catalytic triad, composed of cysteine 223 (C223), histidine 464 (H464), and aspartate 481 (D481), is found and is essential to the function of USP7 (Hu et al., 2002). In the absence of a ubiquitinated substrate, the catalytic triad of USP7

remains in an inactive conformation, as the spatial distance between the deprotonating histidine (H464) and the catalytic cysteine (C223) is too great to support catalysis. Upon binding of a ubiquitinated substrate, conformational rearrangements occur within the catalytic cleft that reposition these residues into proximity, thereby realigning the triad and enabling efficient deubiquitination (Kim et al., 2016; Pozhidaeva & Bezsonova, 2019; Z. Wang et al., 2019). USP7 is activated by substrate-conjugated ubiquitin rather than free ubiquitin. This is because the negatively charged C-terminus of free ubiquitin is unfavourable for interaction in the hydrophobic catalytic cleft, whereas substrate pairing enables proper positioning of the ubiquitin tail for activation(Rougé et al., 2016; Z. Wang et al., 2019). USP7 exists in a dynamic equilibrium between inactive and active conformations. The C-terminal ubiquitin-like domains Ubl4 and Ubl5 play a regulatory role in this process by stabilizing the active state of the catalytic domain, thereby promoting deubiquitination (Kim et al., 2016). The Ubl4–5 domains interact with the switching loop of the catalytic domain at residue W285, which is located near the binding pocket for the substrate ubiquitin C-terminus. This interaction allows the ubiquitin tail to get closer to the catalytic site, thus stabilizing its interaction with the active site and enhancing ubiquitin binding affinity (Kim et al., 2016).

The five ubiquitin-like (UBL) domains of USP7 are located at the C-terminus, spanning residues 564–1102. The catalytic domain is connected to the UBL domains by a 29-residue α-helix, which is thought to contribute to the regulation of USP7's activity state. The UBL domains are arranged in a 2-1-2 organization: UBL1 and UBL2 are positioned together as a pair, followed by a flexible linker that connects to UBL3, which is then separated by another flexible linker from the paired arrangement of UBL4 and UBL5 (Faesen et al., 2011; Z. Wang et al., 2019).

Within UBL2, there is a secondary protein recognition sequence ^{758}DELMDGD^{764}, which recognizes the KxxxK motif on target substrates, where the aspartate residues create an essential salt bridge with the lysine residues, stabilizing the interaction(Yim et al., 2017; Zlatanou et al., 2016). The interaction of substrates at the CTD protein recognition sequence ^{758}DELMDGD^{764} has been characterized with DNMT1, UHRF1 and EZH2, which all possess the Kxxxk motif (Du et al., 2010; Felle et al., 2011; Gagarina et al., 2020).

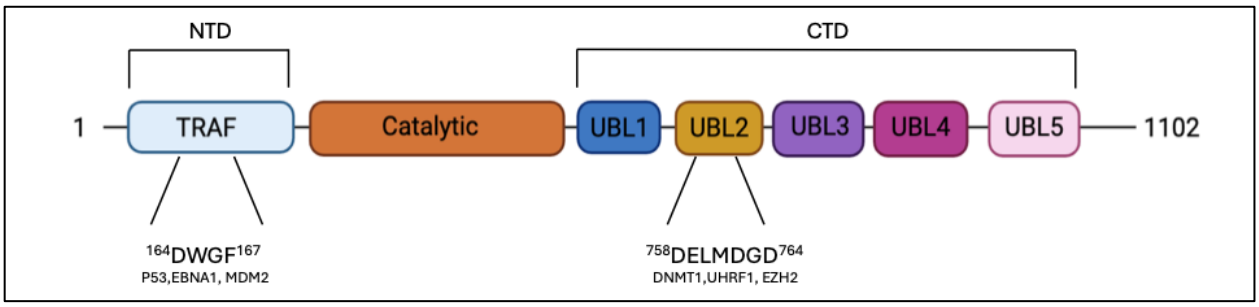

Figure 4. Schematic representation of the domain architecture of USP7.
showing the N-terminal TRAF-like domain, the central catalytic USP domain, and the C-terminal ubiquitin-like (UBL) domains. The TRAF-like domain contains the ^{164}DWGF^{167} motif for substrate binding, while the Ubl2 region provides another substrate interaction site via the ^{758}DELMDGD^{764} motif. Created with BioRender.com.

1.8 USP7's Role in Epigenetic Regulation

USP7 is not only a deubiquitinating enzyme but also an important regulator of epigenetics. It also plays a role in maintaining and modulating histone ubiquitination, supports Polycomb complexes, and stabilizes transcriptional repressors, therefore linking ubiquitin signalling to long-term gene silencing and epigenetic memory. Histone modifications are a crucial regulatory mechanism that determines the chromatin structure and regulates all DNA template-dependent events. One of these modifications is the monoubiquitination of histone H2B on lysine 120 (uH2BK120). This histone modification causes an increase in surface area by

approximately 4800 Å, which allows for the binding of various proteins to the histone, allowing further modifications such as H3K27 methylation (Wojcik et al., 2018). Just as ubiquitination of histone H2B at lysine 120 (uH2BK120) promotes transcriptional activation by increasing nucleosome accessibility, its removal is generally associated with transcriptional repression, as the nucleosomal surface area becomes more compact. USP7 has been identified as an interacting partner of histone H2B and directly catalyzes deubiquitination at lysine 120, thereby contributing to the epigenetic regulation of gene expression (Su et al., 2021). In addition to its role in histone modifications, USP7 also stabilizes and interacts with various chromatin "reader" and "writer" proteins, thereby influencing the activity of key epigenetic regulators (Pozhidaeva & Bezsonova, 2019). Polycomb Repressive Complex 2 (PRC2) is a multi-protein complex composed of "reader" and "writer" proteins, which play a role in the methylation of histone 3 lysine 27 (H3K27). The PRC2 complex mediates the trimethylation on H3K27, which is a canonical epigenetic marker of gene silencing within the cell (Liu & Liu, 2022). Reader proteins from the PRC1 can then recognize and sequester onto the H3K27me3 mark and catalyze the monoubiquitination of H2A on lysine 119, further compacting chromatin and reinforcing transcriptional repression (Ku et al., 2008). EZH2, which is the catalytic subunit of the PRC2, has been identified as a direct substrate of USP7 linking deubiquitination to the stabilization and activity of this critical epigenetic regulator (Gagarina et al., 2020). USP7 directly controls the stability of EZH2 by removing ubiquitin, which in turn does not allow the 26S proteosome to degrade it. The rescued EZH2 can then efficiently catalyze H3K27 trimethylation at target loci, causing transcriptional repression of a plethora of genes, such as FOXO1, which plays a role in proliferation and cell growth. Loss or inhibition of USP7 leads to reduced EZH2 protein levels,

decreased H3K27me3 marks (Su et al., 2021). Similar to its role in stabilizing EZH2 within PRC2, USP7 also regulates the protein stability of RING1B, a core subunit of PRC1. By deubiquitinating RING1B, USP7 prevents its proteasomal degradation, allowing it to function as an E3 ligase and catalyze monoubiquitination of histone H2A at lysine 119 (de Bie et al., 2010). In addition to its interactions with Polycomb Repressive Complexes, USP7 also modulates histone acetylation by deubiquitinating histone acetyltransferases (HATs) and histone deacetylases (HDACs), rescuing them from proteasomal degradation. The HAT TIP60 has been identified as a USP7 substrate. TIP60 acetylates lysine 120 on p53, a modification essential for p53-mediated apoptosis (Dar et al., 2013). USP7 also targets the HDAC SIRT7, a NAD^+-dependent class III deacetylase involved in regulating diverse cellular processes and responding to cellular stresses, such as hypoxia (Jiang et al., 2017). Through these interactions, USP7 contributes to the fine-tuning of acetylation marks on histones and non-histone proteins, further influencing gene expression and chromatin dynamics.

1.9 USP7 and DNA Damage Response

USP7 plays a role in double-strand break (DSB) repair by interacting with key proteins involved in the repair process. There are two methods by which DSB can be repaired, which are either homologous recombination (HR) or non-homologous end joining (NHEJ). Repairs conducted using HR occur during the S and G2 phases of the cell cycle because they require a template, specifically the sister chromatid, whereas NHEJ can occur at any point in the cell cycle, as it does not require a template (Brandsma & Gent, 2012). A key protein in both repair pathways is PHF8, a histone demethylase necessary for recruiting BLM and KU70 to the DSB site (Q. Wang et al., 2016). USP7 is a known DUB for PHF8, stabilizing its levels; moreover, knocking

down USP7 significantly reduces DSB repair efficiency, as the knockdown of USP7 induces a reduction in PHF8 (Q. Wang et al., 2016). Additionally, USP7 regulates MDC1, a protein involved in DSB detection and signalling, where reduced USP7 levels lead to decreased MDC1 levels (Su et al., 2018). MDC1 binds to H2AX, enabling the recruitment of RNF8 and RNF168, which subsequently catalyze K63-linked polyubiquitination, which serves as a scaffold for more DSB repair proteins (Nowsheen et al., 2018). USP7 contributes to this process in two ways: it indirectly controls RNF168 recruitment by stabilizing MDC1, and it directly interacts with RNF168 and its paralog RNF169, deubiquitinating them to regulate their stability (An et al., 2017; Zhu et al., 2015). Another role of USP7 in DSB repair involves its interaction with and stabilization of checkpoint kinase 1 (Chk1), which governs cell cycle checkpoints and facilitates HR repair (Vega et al., 2014).

Another well-studied DNA damage response pathway is the USP7-p53-Hdm2 axis, where research has shown that USP7 can bind to both p53 and Mdm2 (Sheng et al., 2006). The tumour suppressor protein p53 has been called the “guardian of the genome,” as extensive studies have been conducted on its role in preserving genomic stability (Lane & Levine, 2010). The specific genes activated by p53 depend on the type and severity of cellular damage that occurs, which can lead to outcomes such as DNA damage repair or apoptosis (Hager & Gu, 2014). When there is no cellular damage, p53 levels are minimal as p53 is ubiquitinated by the E3 ubiquitin ligase Mdm2. Mdm2 also undergoes autoubiquitination, resulting in its degradation via the 26S-proteasome. However, in the absence of damage, USP7 preferentially deubiquitinates Mdm2. This preferential binding and deubiquitination are facilitated by phosphorylation of USP7 at serine 18 by Chk2, which increases USP7’s affinity for Mdm2 (Khoronenkova et al., 2012).

Consequently, Mdm2 is deubiquitinated and can ubiquitinate p53, marking it for degradation by the 26S proteasome, preventing unnecessary DNA damage responses. Under cellular stress, USP7's role becomes critical because p53 levels must increase to address the cellular stress. To achieve this, USP7-mediated deubiquitination of Mdm2 must be inhibited, permitting Mdm2 degradation and consequently enabling p53 accumulation within the cell. This switch occurs when USP7 is dephosphorylated at serine 18 in an ATM-dependent process by the phosphatase Protein Phosphatase 1G (PPM1G) (Khoronenkova et al., 2012). As a result, USP7 then preferentially binds to and deubiquitinates p53, enabling the DNA damage response to occur as Mdm2 is targeted for degradation via the 26S-proteasome.

1.10 USP7 and Cancer

USP7 has been identified as an interacting partner in many pathways, such as epigenetic regulation, cell proliferation, and DNA damage response. With USP7 regulating these essential pathways, it has emerged as a critical regulator of oncogenic processes (Saha et al., 2023). A well-studied role of USP7 is its regulation of key epigenetic regulators, such as those involved in the polycomb repressive complexes. EZH2, which is the catalytic subunit of PRC2, is deubiquitinated by USP7, which affects the stability of EZH2 (Gagarina et al., 2020). Overexpression of USP7 elevates EZH2 levels, promoting cell proliferation, invasion, and tumour pathogenicity. Conversely, knocking down USP7 leads to a reduction in EZH2 levels, leading to decreased H3K27 hypermethylation, transcriptional repression, and tumour progression (Lee et al., 2020; Zheng et al., 2020). USP7 is overexpressed in T-cell acute lymphoblastic leukemia (T-ALL), where it deubiquitinates and stabilizes NOTCH1 (Shan et al., 2018). NOTCH1 is a transmembrane receptor involved in many cellular processes, including cell

survival, metastasis, proliferation, and differentiation, functioning as a ligand-activated transcription factor (Yamamoto et al., 2014). Upon ligand binding, NOTCH1 is cleaved by ADAM metalloprotease and the γ-secretase complex, releasing intracellular NOTCH1 (ICN1), which then enters the nucleus to activate downstream target genes. Upregulation of ICN1/NOTCH1 occurs in most human T-ALL cases (Weng et al., 2004). USP7 contributes to T-ALL by binding to and stabilizing ICN1 through deubiquitination, thereby suppressing T-ALL cell proliferation (Shan et al., 2018). In summary, USP7 plays a role in tumour progression by stabilizing key regulators such as EZH2 and NOTCH1. These interactions sustain epigenetic repression and signalling pathways that promote and support cancer cell proliferation and progression.

1.11 RNF20

Ring finger protein 20 (RNF20) in complex with RNF40 acts as an E3 ubiquitin ligase, which mediates the monoubiquitination of H2BK120 (Hahn et al., 2012). RNF20 and RNF40 form a heterodimer to fulfill the complete E3 ligase function (Shiloh et al., 2011). In yeast, the E3 ligase is Bre1, whereas in humans, there are two proteins, RNF20/Bre1A and RNF40/Bre1B(Onishi et al., 2024). The three Bre1 (Bre1, RNF20/Bre1A and RNF40/Bre1B) proteins possess a conserved C-terminal RING domain that is critical for their E3 ligase activity, mediating the site-specific monoubiquitination of histone H2B at lysine 120 in humans and the corresponding lysine 123 in yeast. The structure of RNF20 spans 975 residues and can be distinguished by its C-terminal RING domain, N-terminal α-helix and elongated helical regions predicted to form coiled coils (Figure 5) (Foglizzo et al., 2016). The E3 ligase activity of RNF20/RNF40 depends upon its association with its respective specialized E2 Ube2B or Rad6 in yeast (Foglizzo et al., 2016). The RNF20/RNF40 E3 heterodimer coordinates the transfer of the

ubiquitin molecule from the E2 (Ube2B) to the ε-NH_2 lysine on the target substrate. For this transfer to occur, the ring domain of RNF20 is required to stabilize the E2-ub conjugate by interacting with both the ubiquitin and the Ube2B. Once stabilized, the ubiquitin can be transferred to the target substrate lysine(Foglizzo et al., 2016).

RNF20 recruitment to H2B for its ubiquitination has been associated with multiple cellular processes, including the DNA damage response. In the DDR pathway, the knockdown of either RNF20 or RNF40 caused a retardation in the double-strand break repair. In addition, ubiquitination of histone 2B was induced when double-strand breaks were present, and RNF20 was recruited to those double-strand break sites, providing evidence of RNF20 being involved in the DDR pathway (Shiloh et al., 2011). The DDR pathway is one of the many pathways in which RNF20 is engaged; some of the other pathways include hypoxia-induced transcriptional activation, snail-mediated E-cadherin repression and the facilitation of spindle assembly through the stabilization of Eg5 (Duan et al., 2016; Lyu et al., 2024; D. Wang et al., 2020). RNF20 is involved in numerous biological processes, and its dysregulation can act as an intermediary in the development of various carcinomas, including breast cancer, prostate cancer, lung cancer, and clear cell renal cell carcinoma (kidney cancer) (Sethi et al., 2018). Histone 2B (H2B) plays a central role in the cell's transcription of many key genes. The regulation of H2B activity requires precise ubiquitination and deubiquitination processes, positioning RNF20 as a critical factor in gene transcriptional control.

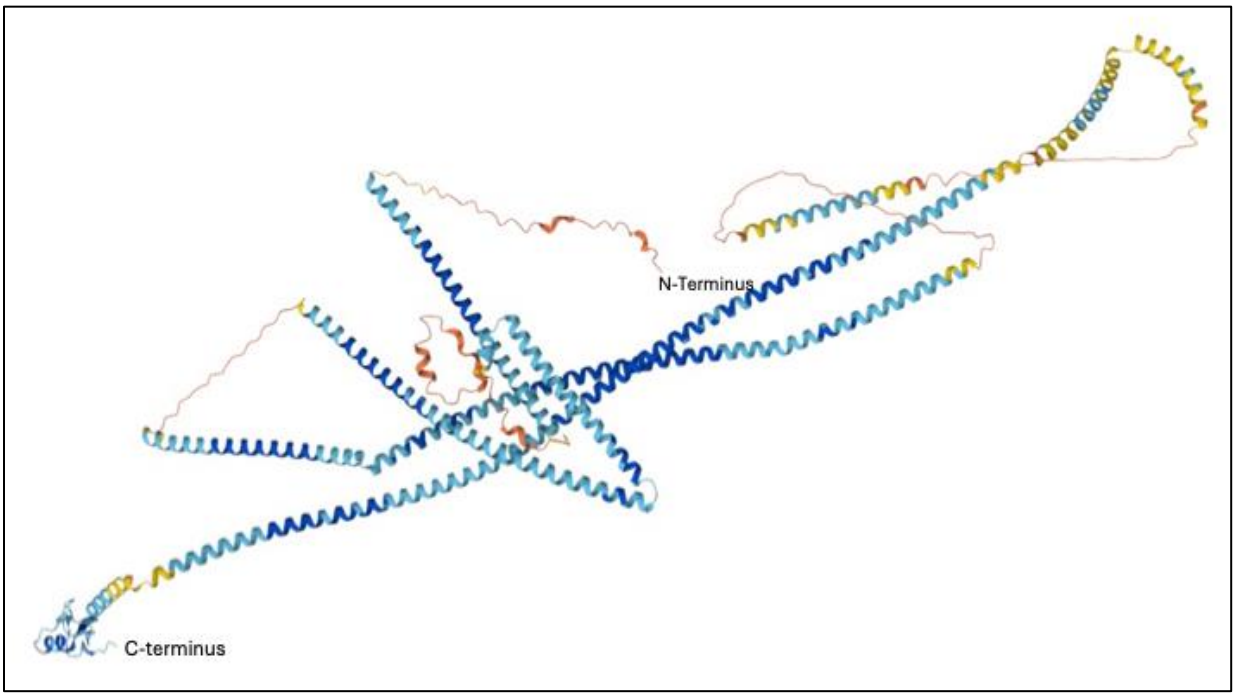

Figure 5. Predicted structure of human RNF20.
Generated by AlphaFold, modified to indicate the N-terminus and C-terminus (Jumper et al., 2021; Varadi et al., 2022)

1.12 Research Rationale and Objectives

USP7 is known for its deubiquitination of uH2BK120, while RNF20 is responsible for ubiquitinating the same site on H2B. However, there is a lack of research into any possible interaction between USP7 and RNF20. Considering their opposing effects on H2B, USP7 potentially regulating RNF20 could create an interesting dynamic in controlling H2B ubiquitination. Additionally, given RNF20's role in various pathways and the possibility of USP7 influencing these through RNF20, there is a compelling rationale to further investigate their interaction.

A bioinformatics search utilizing Eukaryotic Linear Motif (ELM) unveiled an ASSS motif within RNF20, a motif previously observed to promote protein interaction with USP7, which has been reported for RAD18 and 53BP1(Yim et al., 2017; Zlatanou et al., 2016). The motif identified

in RNF20 supports the possibility of its interaction with USP7. Additionally, it was found that RNF20 undergoes ubiquitination by Smurf2, indicating the potential for RNF20 to undergo deubiquitination (Blank et al., 2012). Furthermore, there is a research gap in the proteins responsible for the deubiquitination of RNF20. Therefore, it is postulated that USP7 plays a role in the stability of RNF20 by catalyzing its deubiquitination. The objectives of the research project were to determine if there is any interaction between USP7 and RNF20 and to subsequently establish a role for this interaction. The next steps entailed determining if the interaction has any effects on the stability or function of RNF20.

Chapter 2: Materials and Methods

2.1 Plasmids

Plasmids that were used for Mammalian transfection were pcDNA3/FLAG-Empty Vector, pcDNA3/Myc-USP7 and pcDNA3/Myc-C233S Mutant (Catalytically inactive USP7) were previously described (Pfoh et al., 2015), pCMV3-FLAG-RNF20 (Sino Biological, HG13962-NF) and pcDNA3/HA-Ub (Addgene, 18712).

2.2 Transfection and Mammalian Cell Culture

Human colorectal carcinoma HCT116 parental, HCT116 USP7$^{-/-}$ KO, and MCF7 breast cancer cell lines were grown in McCoy's media (Wisent Inc, 317010 CL) supplemented with 1% penicillin-streptomycin (Wisent Inc, 420201) and 10% fetal bovine serum (Gibco, 12483020). Human embryonic kidney cells (HEK293T) were grown in DMEM (Wisent Inc, 319005 CL) supplemented with 1% penicillin-streptomycin and 10% fetal bovine serum. The cells were grown in an incubator at 37 °C and 5% CO_2. Transfections were conducted using Polyjet™ in vitro DNA transfection reagent (SignaGen Laboratories) following the manufacturer's instructions.

2.3 SDS-Page Gel and Western Blotting

The SDS-PAGE gel was conducted using a 4% acrylamide stacking gel and a 10% acrylamide running gel. The gel was run at 120 volts for an hour, followed by a transfer using an activated PVDF membrane for 1 hour and 45 minutes with 100 volts at 4 °C. The membrane was blocked post-transfer using 5% milk with PBST (NaCl 137 mM, KCl 2.7 mM, Na2HPO4 10mM, KH2PO4 1.8mM, 0.1% Tween-20) for one hour with agitation using a shaker, followed by incubation with primary antibodies overnight at 4 °C on a rocker. After the overnight incubation,

the membrane was washed three times using PBST for five minutes each, followed by incubation with secondary antibodies at room temperature on a rocker for one hour. The membrane was then washed three times for 15 minutes each using PBST after the incubation with the secondary antibodies. The membranes were imaged on the Azure 280 (Azure Biosystems) after incubating in ECL (Cytiva, GERPN2236) for five minutes.

2.4 Antibodies

The primary antibodies used for immunoblotting were anti-GAPDH (0411) mouse (Santa Cruz Biotechnology Inc., 47724), anti-GAPDH(14C10) rabbit (Cell Signalling Technology, 2118), anti-USP7 (Bethyl Laboratories, A300-033A), anti-Myc (Invitrogen, 2243074), anti-HA tag(C29F4) rabbit (Cell Signalling Technology, 3724), anti-FLAG tag (Sigma Aldrich, F1804), anti-RNF20(Cell Signalling Technology, D6E10), and HRP-conjugated goat polyclonal mouse IgG (Thermofisher, 31430). The secondary antibodies used were anti-mouse IgG HRP-conjugated goat polyclonal (ThermoFisher, 31430) and anti-rabbit IgG HRP-linked (Cell Signalling Technology, 7074).

2.5 Cell Harvesting, Lysis and Sample Preparation

To harvest the HCT116, MCF7 and HEK293T cells, the cells were first washed in cold PBS (Wisent), followed by the addition of 0.25% trypsin-EDTA (Gibco, 325542) for five minutes in a 37°C incubator to detach the adherent cells. The trypsin was neutralized using McCoy's or DMEM media, and the cells were collected by centrifuging the cells in 15 ml Falcon tubes at 200 x g for five minutes. The cells were then resuspended in cold PBS and placed in 1.5 ml microtubes. The cells were lysed using either NP-40 lysis buffer (50 mM Tris [pH 7.5], 500 mM NaCl, 5 mM Imidazole, and 5% Glycerol) or RIPA lysis buffer (150mM NaCl, 50mM TRIS-HCl [pH 7.4], 1% NP-40, 0.5% Sodium deoxycholate and 0.1% SDS) with the protease inhibitors 1mM

PMSF, 1mM benzamidine and 1x complete protease inhibitor cocktail (Roche cOmplete ULTRA Tablets, 5892970001). The resuspended cells were chemically lysed by rotating for 45 minutes at 4°C. After the lysing process, the supernatant was collected after centrifuging the lysed cells at 17,000 x g for 15 minutes at 4°C. To prepare the samples for Western blot analysis, the protein concentrations were determined using Pierce™ BCA Protein Assay Kit (ThermoFisher, 23227) according to the manufacturer's protocol. 20 µg of lysate was prepared by boiling for 5 minutes at 100 °C in 1x SDS-PAGE loading buffer (250 mM Tris-Cl, pH 6.8, 2% (w/v) SDS, 30% (v/v) glycerol, 0.5 M DTT, 0.05% (w/v) bromophenol blue, 5% β-mercaptoethanol) before being loaded on an SDS-PAGE gel.

2.6 Co-Immunoprecipitation

In order to conduct the co-immunoprecipitation (co-IP), 1000 µg of protein was used per condition. The mammalian lysates were first incubated with 2µl of either mouse anti-USP7 antibody or Mouse IgG (Thermofisher, 31430) overnight at 4 °C while rotating. On the following day, 50 µl of Protein A/G beads PLUS-agarose bead (Santa Cruz Biotechnology Inc, sc-2003) were washed 3 times with PBS before being blocked using 5% BSA in PBS for 1 hour with rotation at 4 °C. Post blocking, the beads were washed twice with PBS and once with lysis buffer, then incubated with the mammalian lysate for 2 hours, rotating at 4 °C. The beads were then washed 4 times with PBS before being boiled for 5 minutes in 1x SDS-PAGE loading buffer.

2.7 Cycloheximide Chase

HCT116 parental and HCT116 USP7$^{-/-}$ KO cells were cultured to 80% confluency before being treated with 50 µg/ml of cycloheximide (Sigma-Aldrich, C4859). Cells were then harvested

at 0, 2, 4, 8, 16, 24-hour time points for both cell lines. Following this, the cells were lysed and prepared for a Western blotting as previously described.

2.8 Deubiquitination Assay

To conduct the deubiquitination assay, HEK293T cells were co-transfected with FLAG-RNF20, HA-ubiquitin (HA-Ub), and either parental USP7 (Myc-USP7) or catalytic mutant USP7 (Myc-C233S mutant). 24 hours post-transfection, the cells were treated with 40 µM of MG132(EMD Millipore, 474790) for 4 hours before being harvested. The cells were then lysed, and inputs were prepped for each condition. Additionally, 1000 µg of protein was incubated with 1x TBS (150 mM NaCl, and 20 mM Tris [pH 7.5]) washed ANTI-FLAG® M2 Magnetic Beads (Millipore, M8823) at 4 °C, rotating overnight. After overnight incubation, the beads were washed three times with TBS for 5 minutes each, rotating at 4 °C. Following this, the beads were boiled in 1x SDS-PAGE loading buffer for 5 minutes to prepare them for western blot analysis.

Chapter 3: RESULTS

3.1 Identification of RNF20 as a potential interacting partner for USP7

The N-terminus TRAF/MATH domain of USP7 contains the ^{164}DWGF^{167} motif, which is known to mediate substrate recognition by binding the consensus sequence P/A/ExxS. To identify RNF20 as a potential substrate for USP7, a search for human proteins with the P/A/ExxS motif was performed, followed by analysis of the protein sequences using UniProt, BLAST sequence alignment, and the Eukaryotic Linear Motif (ELM) resource. This bioinformatic analysis revealed that RNF20 contains an ASSS motif, which resembles the USP7 substrate consensus sequence and therefore may bind to USP7. To further investigate this interaction, a sequence alignment was conducted with proteins containing the P/A/ExxS motif that are known to interact with USP7 at the DWGF binding pocket (Figure 6). The proteins used in the alignment included p53, MDM2, CDK8, BMI1, and 53BP1. All these proteins contained either Proline (P), Alanine (A), or Glutamic acid (E) at the first position, as the USP7 substrate consensus sequence allows variability between the three residues at the first position, followed by two variable residues, and ending with a conserved Serine (S). Based on this conserved motif, the presence of the ASSS sequence in RNF20, and its similarity to known USP7 substrates, we pursued RNF20 for further investigation as a potential USP7 interactor.

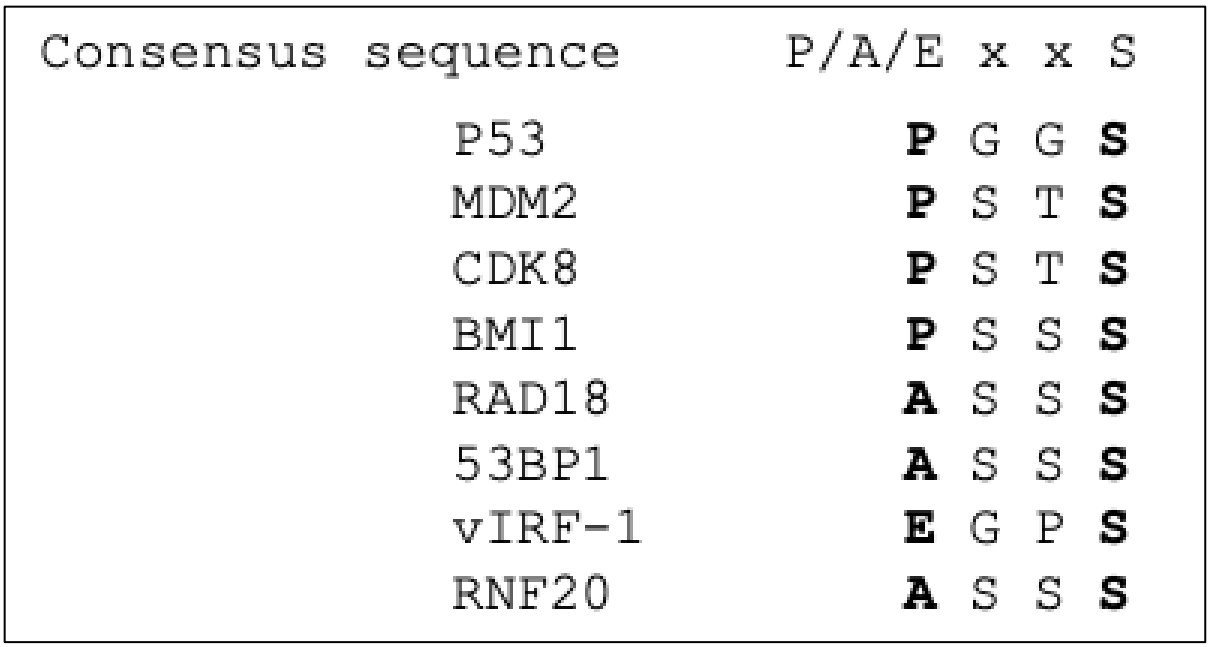

Figure 6. Predicted USP7 interaction motif in RNF20.
Sequence alignment comparing a candidate USP7-binding region in RNF20 with the USP7 consensus motif defined in known substrates.

3.2 Does USP7 Interact with RNF20?

To determine if USP7 and RNF20 interact under endogenous conditions, a co-immunoprecipitation(co-IP) assay was conducted in three different cell lines, which were MCF7, HCT116 and HEK293T (Figure 7). Whole-cell lysates were immunoprecipitated using an anti-USP7 antibody overnight, and the resulting complexes were captured with protein A/G agarose beads. After extensive washing to remove non-specific proteins, the immunocomplexes were analyzed via western blotting. As shown in Figure 7, an interaction between USP7 and RNF20 was characterized in all three cell lines (A) MCF, (B) HCT116 and (C) HEK293T. Importantly, RNF20 was absent in the IgG control lanes, confirming the specificity of the interaction, supporting the conclusion that USP7 associates with RNF20 under endogenous conditions.

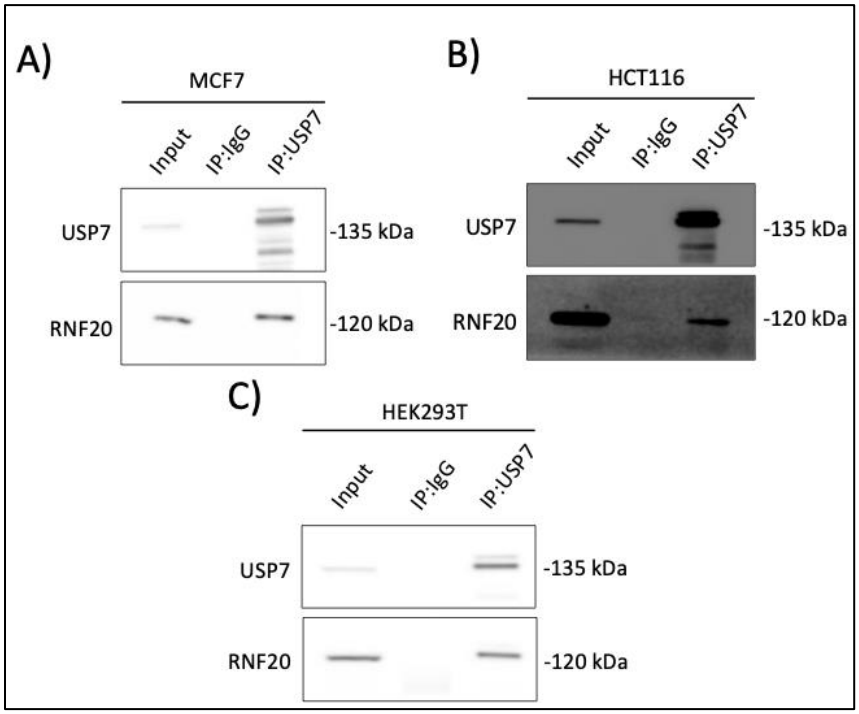

Figure 7. Endogenous co-immunoprecipitation of USP7 with RNF20 in different cell lines.
(A) MCF7, (B) HCT116, and (C) HEK293T cell lysates were subjected to immunoprecipitation with anti-USP7 antibody or control IgG. The resulting immunocomplexes were analyzed by immunoblotting to detect the endogenous interaction between USP7 and RNF20.

3.3 Does USP7 affect RNF20 stability?

To assess if USP7 affects the stability of RNF20, a western blot on the lysates from two different cell lines was conducted (Figure 8A). The two cell lines used were the parental HCT116 cell line, which contains fully functional USP7, or the HCT116 USP7$^{-/-}$ KO cell line, where USP7 has been knocked out. The Western blot revealed a robust difference in the protein levels of RNF20 in the two cell lines, with the knockout cell line displaying less RNF20 (Figure 8A). To further analyze the Western blots, a statistical analysis was conducted in which the protein signal was quantified using ImageJ, following which the signal was normalized to GAPDH, the loading control. The statistical analysis was conducted on 3 replicates of the experiment, with the data displayed as mean ± SEM (Figure 8B). The RNF20 mean fold change in the HCT116 parental cells was 0.7337 ± 0.028, whereas in the HCT116$^{-/-}$ KO, the mean fold change was 0.4241 ± 0.061. A two-tailed Student's T-test was performed, giving a t-statistic of 7.95, yielding a p-value of 0.0014, indicating that there is a statistically significant difference in the RNF20 protein concentration between HCT116 parental cells and the HCT116 USP7$^{-/-}$ KO cells. This result showed that the presence of USP7 plays a role in the stability of RNF20.

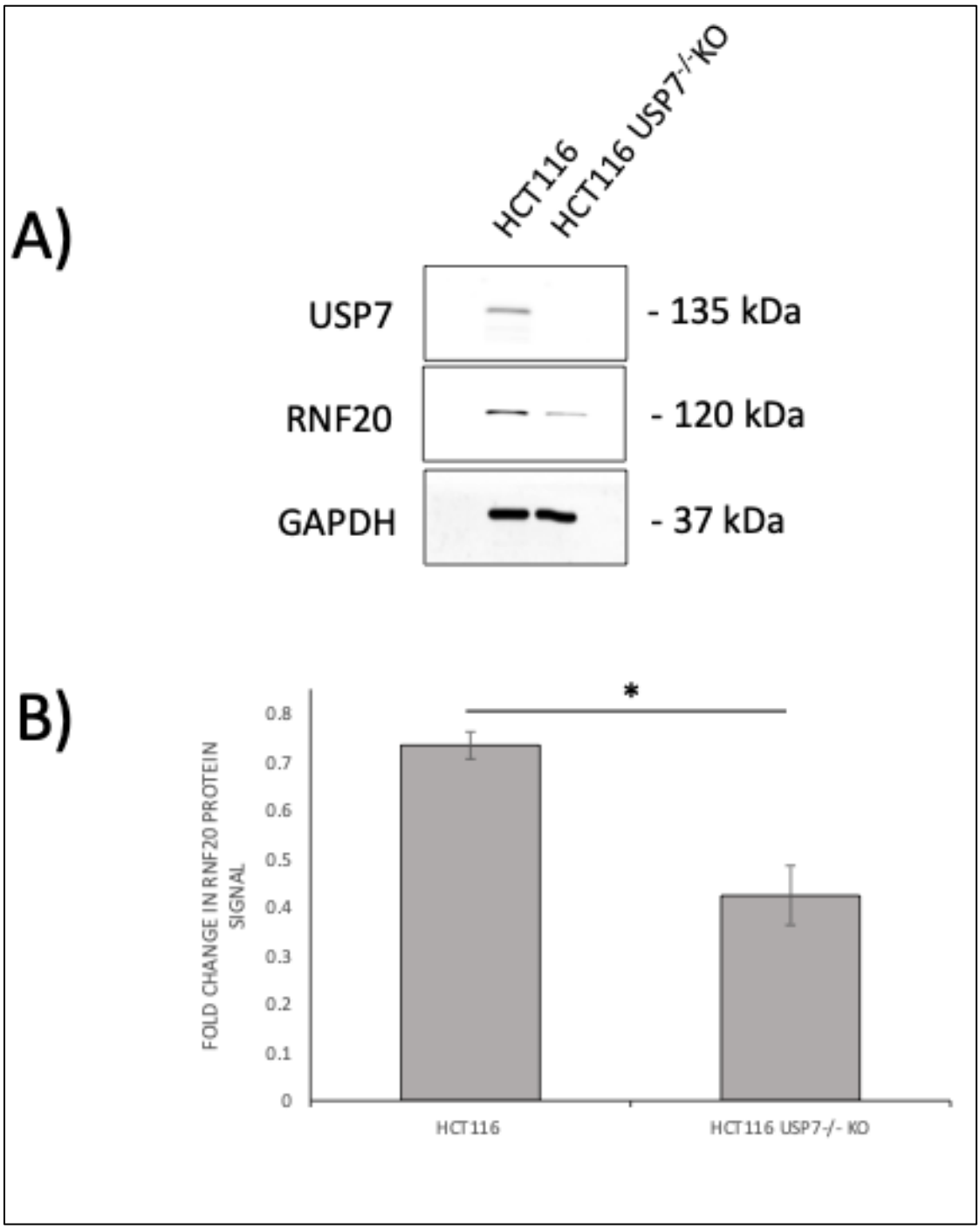

Figure 8. Western blot analysis of RNF20 expression in parental and USP7 knockout HCT116 cells.

A) Whole cell lysates from parental (WT) and USP7 knockout (USP7$^{-/-}$ KO) HCT116 cells were analyzed by Western blot using antibodies against USP7, RNF20 and GAPDH.

(B) RNF20 band intensities were quantified using ImageJ from independent experiments. Data are presented as mean ± SEM. Statistical significance was determined using a two-tailed Student's *t*-test (n=3).

3.4 USP7 Reconstitution in HCT116 USP7$^{-/-}$KO Cells

To assess the functional relevance of USP7 catalytic activity on the stability of RNF20, the next experiment was a reconstitution of parental USP7 or the catalytically inactive form of USP7 (C233S-mutant) in the HCT116 USP7$^{-/-}$ KO cells (Figure 9A). The results of the conducted western blot displayed an increase in RNF20 protein levels in the knockout cells that had parental USP7 transfected into them. In contrast, the cells transfected with the C233S mutant displayed analogous results to those of the protein level of RNF20 in the knockout cells (Figure 9A). To further analyze the Western blots, a statistical analysis was conducted in which the protein signal was quantified using ImageJ for three replicates of the experiment, following which the signal was normalized to GAPDH, the loading control. The data were then analyzed using a one-way ANOVA, followed by Tukey's post-hoc test to identify which experimental groups differed significantly from each other. The data were displayed as mean ± SEM (Figure 9B). The mean RNF20 fold change was 0.856 ± 0.105 in HCT116 parental cells, 0.298 ± 0.037 in HCT116 USP7$^{-/-}$ KO cells, 0.426 ± 0.007 in HCT116 USP7$^{-/-}$ KO cells reconstituted with Myc-USP7, and 0.113 ± 0.039 in HCT116 USP7$^{-/-}$ KO cells expressing the Myc-C233S catalytic mutant (Figure 9B). Tukey's post-hoc test revealed significant differences in RNF20 levels between HCT116 parental cells and USP7$^{-/-}$ knockout cells expressing the Myc-C233S catalytic mutant ($p = 0.000096$), indicating a highly significant reduction. A significant difference was also observed between parental cells and USP7$^{-/-}$ knockout cells ($p = 0.0007$). Additionally, USP7$^{-/-}$ knockout cells reconstituted with Myc-USP7 differed significantly from USP7$^{-/-}$ KO cells expressing the Myc-C233S catalytic mutant ($p = 0.0237$). These results indicate that RNF20 stability is linked to the catalytic activity of USP7 and that the C233S mutant fails to regulate the stability of RNF20.

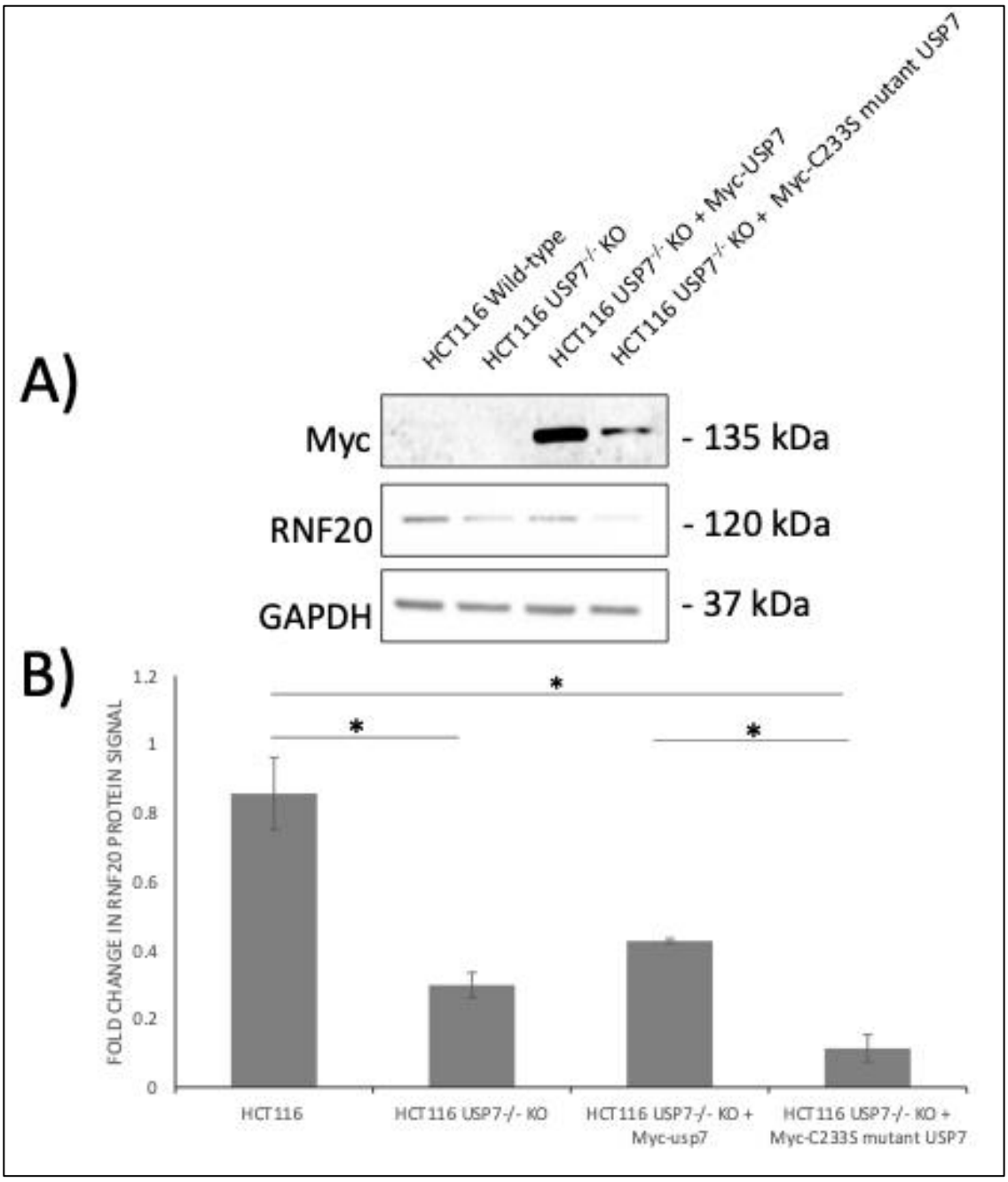

Figure 9. Analysis of RNF20 expression in HCT116 USP7 knockout (KO) cells transfected with parental or mutant USP7.

(A) HCT116 USP7 KO cells were transfected with no plasmid (negative control), parental USP7 (Myc-USP7), or a catalytically inactive mutant USP7 (Myc-C233S mutant). RNF20 protein levels were assessed by immunoblotting.

(B) Quantification of RNF20 protein levels. Band intensities were measured using ImageJ, normalized to loading controls, and plotted as mean ± SEM. Statistical significance was determined by one-way ANOVA followed by Tukey's post-hoc test (n=3).

3.5 Analysis of RNF20 Levels upon Overexpression of Parental and Catalytic Mutant USP7

The next experiment conducted was an overexpression experiment where there was transfection of FLAG-RNF20 with either Myc-USP7 or Myc-C233S mutant USP7 in HCT116 parental cells (Figure 10). The results of the subsequent western blot revealed an increase in RNF20 protein levels in Myc-USP7-transfected cells, whereas there was a decrease in RNF20 levels in cells transfected with the Myc-C233S mutant (Figure 10A). To further analyze the Western blots, protein band intensities from three replicates were quantified using ImageJ, following which the signal was normalized to GAPDH, the loading control. The data were then analyzed using a one-way ANOVA, followed by Tukey's post-hoc test to identify which experimental groups differed significantly from each other. The data were displayed as mean ± SEM (Figure 10B). Quantification of RNF20 protein levels revealed a mean fold change of 0.618 ± 0.031 in HCT116 parental cells. In cells transfected with Myc-USP7, the mean fold change increased to 0.945 ± 0.066, whereas transfection with the catalytically inactive Myc-C233S mutant resulted in a reduced mean fold change of 0.468 ± 0.103. The conducted One-way ANOVA revealed that there were statistically significant differences between the experimental groups ($p<0.05$). The Tukey's post hoc test showed that there was a significant difference in RNF20 band intensity between the HCT116 parental cells and the parental cells transfected with Myc-USP7 ($p=0.044$). In addition, there was a statistically significant difference between the Myc-USP7-transfected cells and the Myc-C233S mutant-transfected cells ($p=0.008$). These results show that RNF20 protein levels are increased upon USP7 overexpression and reduced in the presence of the catalytically inactive C233S mutant.

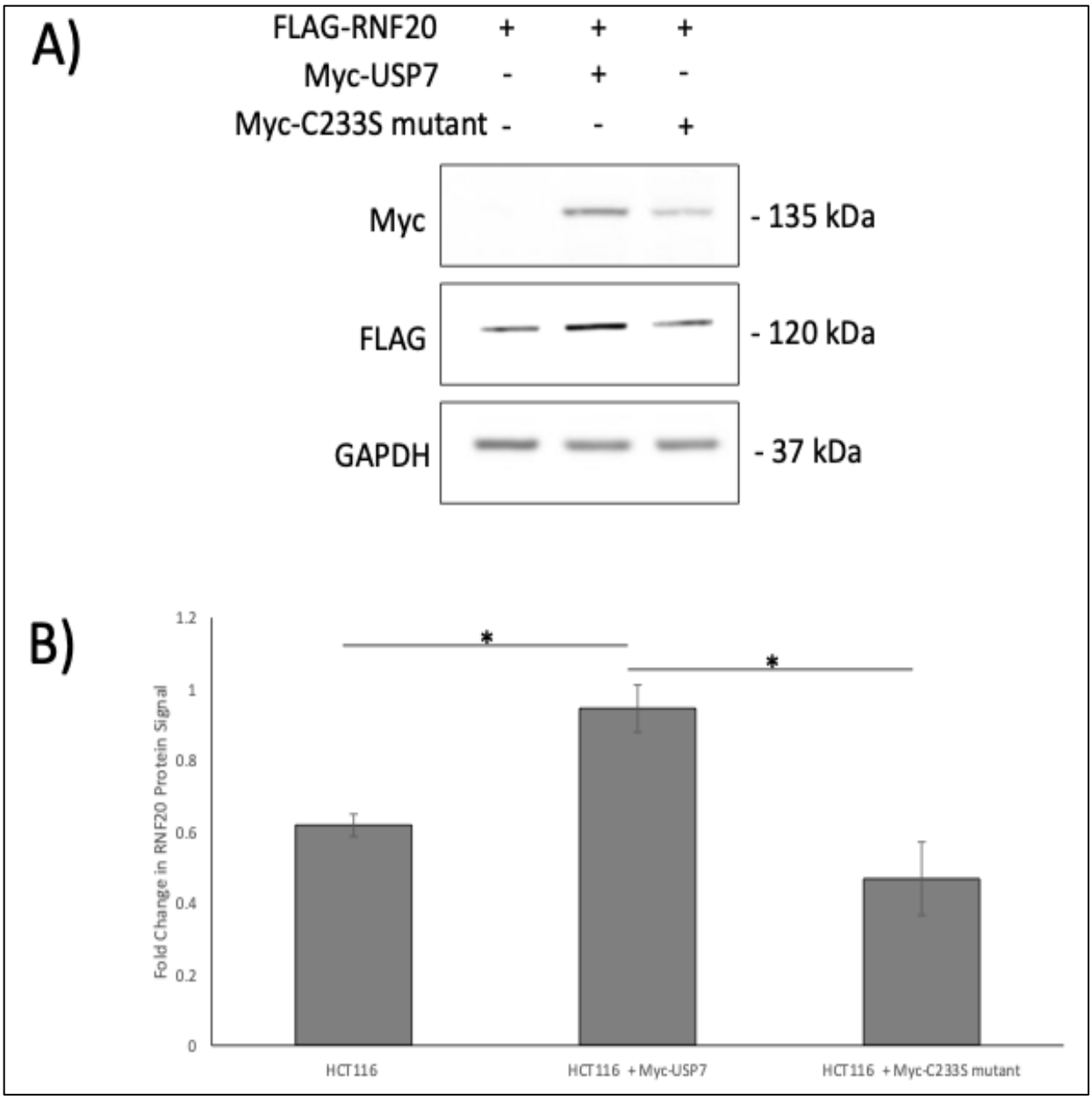

Figure 10. Overexpression of myc-USP7 and the catalytic mutant (Myc-C233S mutant) with FLAG-RNF20 in HCT116.

A) HCT116 cells were transfected with 3 μg of either Myc-USP7 or the catalytically inactive USP7 mutant (Myc-C233S mutant) with 3 μg of FLAG-RNF20. Cell lysates were analyzed by Western blot using antibodies against FLAG, USP7, and GAPDH.

B) Quantification of FLAG-RNF20 protein levels. Band intensities were measured using ImageJ, normalized to GAPDH, and plotted as mean ± SEM. Statistical significance was determined by one-way ANOVA followed by Tukey's post-hoc test (n=3).

3.6 Assessment of RNF20 Degradation in the Presence and Absence of USP7

To assess the effect of USP7 on RNF20 protein stability, a cycloheximide chase was performed on HCT116 parental and HCT116 USP7 $^{-/-}$ knockout cells (Figure 11). Cycloheximide was used to inhibit protein synthesis, enabling the analysis of protein stability over time. Cells were harvested at 0, 2, 4, 8, 16, and 24 hours during the 24-hour time course, and RNF20 protein levels were examined using Western blotting (Figure 11A). Protein levels were quantified with ImageJ and normalized to GAPDH. To determine half-life values, protein levels were normalized to the time-zero value to generate relative decay plots (Figure 11B). RNF20 levels remained relatively stable in parental HCT116 cells, indicating slower degradation with a half-life of 41.3 hours ± 7.95 hours. Conversely, RNF20 levels declined progressively in USP7 knockout cells, suggesting reduced stability in the absence of USP7, with a half-life of 10.2 hours ± 2.42 hours (Figure 11B). These findings are consistent with the overexpression data, supporting the conclusion that USP7 stabilizes RNF20 dependent on its catalytic activity.

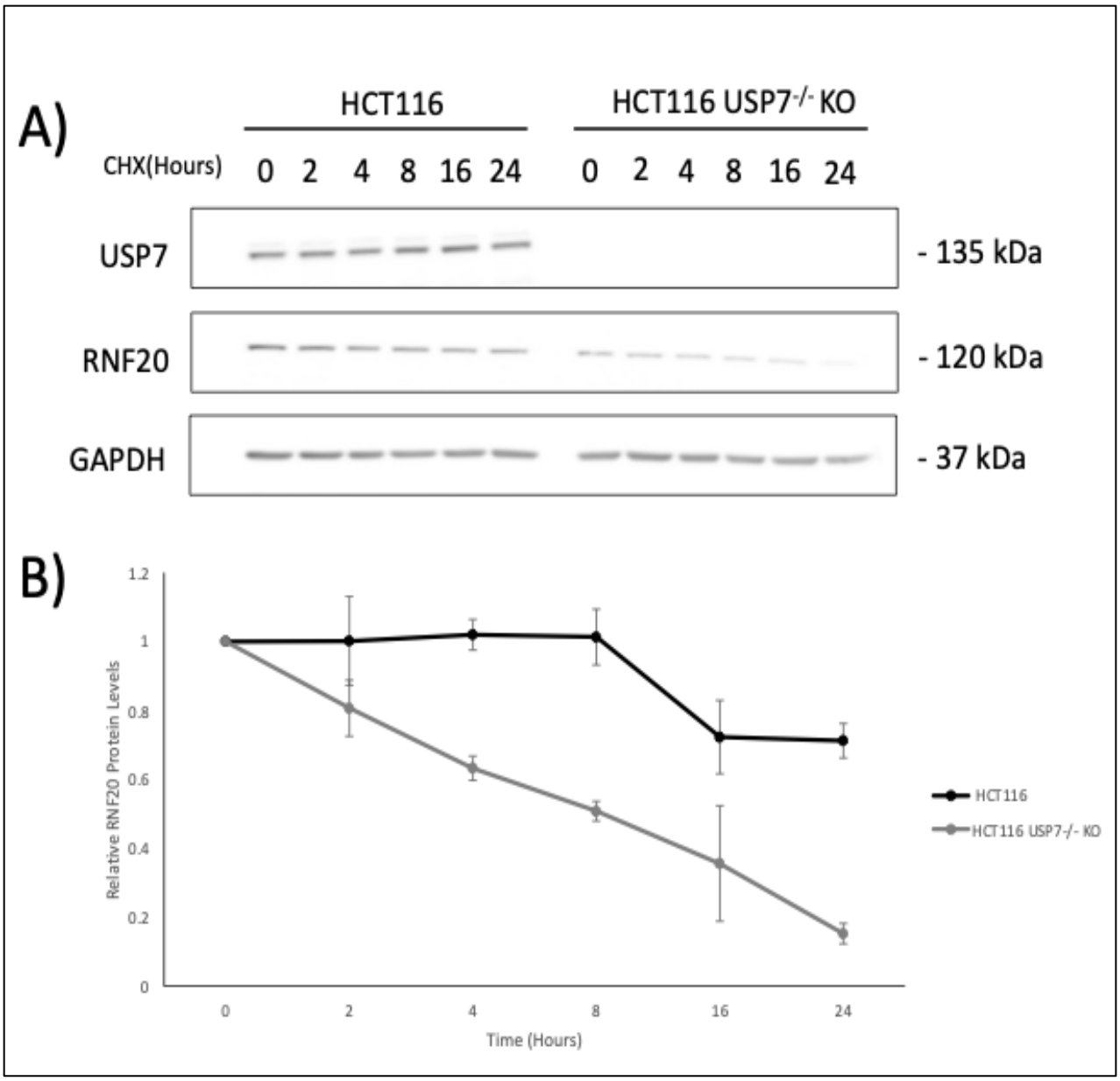

Figure 11. Cycloheximide chase assay in parental and USP7 knockout HCT116 cells.
(A) Western blot analysis of RNF20 protein stability in parental (WT) and USP7 knockout (USP7^{-}/$^{-}$) HCT116 cells following cycloheximide (50 µg/ml) treatment. Cells were harvested at 0, 2, 4, 8, 16, and 24 hours. GAPDH was used as a loading control.
(B) Quantification of RNF20 protein levels over time, normalized to GAPDH, and plotted as a protein decay curve. Data represent mean ± SEM (n=3).

3.7 How does USP7 modulate RNF20 stability?

To determine whether USP7 directly regulates RNF20 stability through deubiquitination, a deubiquitination assay was performed. FLAG-RNF20 and HA-Ub were co-expressed with either Myc-USP7 or the catalytically inactive Myc-C233S mutant and treated with 40 µM of MG132. Subsequently, a co-immunoprecipitation using ANTI-FLAG® M2 Magnetic Beads was conducted, and the HA-Ub was detected by western blotting using anti-HA antibody. The cells transfected with Myc-USP7 showed higher RNF20 deubiquitination compared to the cells not transfected with Myc-USP7 in lane two. Whereas those transfected with the Myc-C233S mutant exhibited lower levels of deubiquitination as compared to the cells transfected with Myc-USP7 in lane three (Figure 12). These results suggest that USP7 stabilizes RNF20 by catalyzing the removal of ubiquitin chains, thus preventing its degradation via the proteasomal pathway.

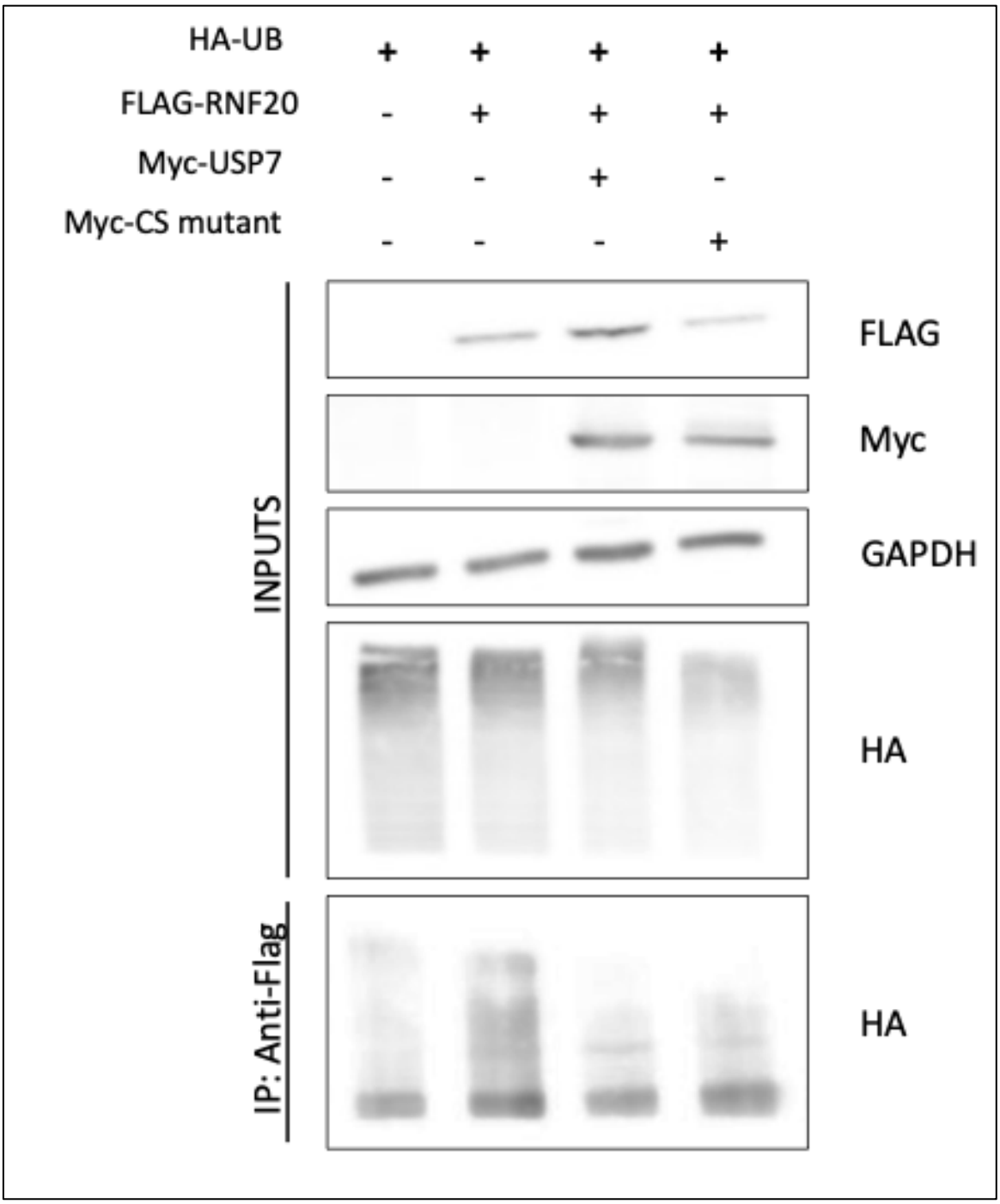

Figure 12. Deubiquitination assay in HEK293T cells using FLAG-tagged RNF20, HA-tagged ubiquitin, and USP7 constructs.

HEK293T cells were co-transfected with FLAG-tagged RNF20, HA-tagged ubiquitin (HA-Ub), and either parental USP7 (Myc-USP7) or catalytic mutant USP7 (Myc-C233S mutant). Additionally, the cells were treated with 40 µM of MG132. FLAG-RNF20 was immunoprecipitated, and ubiquitination levels were assessed by Western blot using anti-HA antibodies. Total input levels of USP7, FLAG-RNF20, and loading control GAPDH were also analyzed (n=3).

Discussion

The project aimed to identify the possible interaction between RNF20, which is an E3 ligase responsible for the monoubiquitination of histone H2B and USP7, a ubiquitin-specific protease which has diverse roles in the cell, such as epigenetic regulation, DNA damage response and oncogenic processes. Using a combination of biochemical and functional assays, including endogenous co-immunoprecipitation, comparing parental and USP7 knockout HCT116 cells, reconstitution assay, overexpression with USP7 or the catalytic mutant USP7, cycloheximide chase and a deubiquitination assay, our findings provide evidence that USP7 interacts with RNF20 and affects the stability of RNF20 through its deubiquitinating activity, thereby stabilizing it and preventing 26S proteasome-dependent degradation.

Endogenous Interaction of USP7 and RNF20

The prediction of the interaction between USP7 and RNF20 stems from two observations. The first being that RNF20 contains an ASSS motif, a short linear sequence that has previously been seen in proteins such as RAD18 and 53BP1 (Yim et al., 2017; Zlatanou et al., 2016) (Figure 6). This motif provided a structural rationale to hypothesize the interaction between USP7 and RNF20. Second, RNF20 is known to be ubiquitinated by the E3 ligase Smurf2 (Blank et al., 2012). However, to date, no deubiquitinating enzyme has been identified that may counteract this ubiquitination. Together, these findings suggest that there should be a deubiquitinase for RNF20, with USP7 being a strong candidate for this role. The identification of the ASSS motif present within RNF20 is significant as it provides the structural basis of how USP7 can recognize and stabilize RNF20. The observation is like that seen in many proteins containing the P/A/ExxS motif, such as RAD18, 53BP1, p53, MDM2 and vIRF-1, where those

proteins interact with USP7 at the DWGF motif within the peptide binding pocket in the N-terminal domain. With all the cellular proteins containing the P/A/ExxS motif, USP7 plays a role in maintaining their stability. Through the interaction with the ASSS binding motif, USP7 will likely be able to recognize and bind RNF20. As a result of this binding, USP7 may be able to deubiquitinate RNF20, thereby preventing its degradation via the 26S proteasome.

Consistent with the prediction, endogenous co-IP experiments provided experimental support to the prediction of interaction between USP7 and RNF20 (Figure 7). The endogenous co-IP demonstrates a physical association between RNF20 and USP7 under physiological conditions. Importantly, this interaction was seen in three different cell lines, which were MCF7, HCT116 and HEK293T. The reproducibility of the interaction in three different cell lines indicates that the interaction is not a condition-specific or tissue-specific interaction, suggesting that it is a physiologically relevant interaction across diverse cell types. This finding is significant as it establishes the interaction between USP7 and RNF20, allowing for further investigation into how the interaction plays a role in the stability of RNF20 and its downstream functions.

USP7 Catalytic Activity is essential to RNF20 Stability

In order to assess the functional relevance of the interaction between USP7 and RNF20, a comparison of RNF20 protein abundance in HCT116 parental cells and HCT116 USP7$^{-/-}$ KO cells was conducted (Figure 8). Notably, the absence of USP7 in the HCT116 USP7$^{-/-}$ KO cells resulted in a significant reduction in RNF20 protein abundance relative to its abundance in the parental HCT116 cells, indicating that the presence of USP7 is required for the maintenance of RNF20 stability under physiological conditions. These findings are consistent with the general role of

deubiquitinases in counteracting ubiquitin-dependent proteasomal degradation and highlight USP7 as an important regulator of RNF20 stability.

The next experiment conducted was to directly test if the reintroduction of USP7 into the HCT116 USP7$^{-/-}$ KO cells could restore RNF20 abundance. To further determine whether this effect is due to the catalytic activity, HCT116 USP7$^{-/-}$ KO cells were reconstituted with either USP7 wild-type (Myc-USP7) or C233S catalytic mutant (Myc-C233S mutant) (Figure 9). Re-expression with the wild-type USP7 displayed an increase in the RNF20 protein abundance as compared to the control Knockout cells that had been transfected with an empty vector, confirming that USP7 is both necessary and sufficient to stabilize RNF20. In contrast, the C233S mutant USP7, which is catalytically inactive and cannot therefore deubiquitinate substrates due to the mutated catalytic site, failed to rescue RNF20 protein levels. This result strongly suggests that the enzymatic deubiquitinating activity of USP7 is required for RNF20 stabilization. Hence, the interaction between USP7 and RNF20 alone is not sufficient in conditions where there is a loss of the catalytic activity.

The third experiment aimed to further analyze the stability of RNF20 by overexpressing RNF20 in the HCT116 parental cells with the co-transfection of either USP7 wild-type (Myc-USP7) or C233S catalytic mutant (Myc-C233S mutant) (Figure 10). This approach allowed us to directly assess whether co-expression with the catalytically active USP7 could increase RNF20 protein abundance and whether the catalytically inactive USP7 would hinder this effect. In the cells expressing the wild-type USP7, RNF20 protein abundance was significantly higher than that of the HCT116 parental cells, as well as the cells that were co-transfected with the C233S mutant USP7. The increase in RNF20 abundance demonstrated in the cells transfected with the

wild-type USP7 and the lack of RNF20 abundance in the cells transfected with the C233S mutant USP7 further confirms that USP7 being present and catalytically active is essential to the stabilizing effect on RNF20.

Collectively, the three experiments conducted were the parental and USP7$^{-/-}$ knockout HCT116 cell comparison, rescue with either the wild-type or C233S mutant USP7, and RNF20 overexpression with the USP7 variants, with the results suggesting a model where USP7 functions as a critical regulator of RNF20 by protecting it from proteasomal degradation by deubiquitinating it. These results provide insight into how RNF20 is post-transcriptionally regulated and adds to the fact that USP7 is a key chromatin regulator. Since RNF20 is an E3 ligase responsible for histone H2B monoubiquitination, USP7, playing a role in its stability, may have broad implications in transcriptional regulation and DNA damage response.

USP7 Prolongs RNF20 Stability

To allow us to analyze the effect of USP7 on RNF20 protein turnover, a cycloheximide chase was conducted to monitor the protein levels of RNF20 over time (Figure 11). In the HCT116 parental cells, RNF20 displayed a relatively stable half-life with a gradual degradation following the treatment with cycloheximide to inhibit protein synthesis. In comparison, the RNF20 protein levels in the HCT116 USP7$^{-/-}$ KO cells declined significantly faster, indicating an accelerated turnover rate in the absence of USP7. The difference in decay rates provides strong evidence that USP7 is necessary to prolong the half-life of RNF20. This increase in half-life can be linked to the deubiquitinating function of USP7, as it stabilizes RNF20 by counteracting the ubiquitin-dependent degradation. The results from the cycloheximide chase further reinforce the fact that USP7 plays a critical role in maintaining RNF20 protein homeostasis, rather than

having an indirect effect. In addition, the cycloheximide chase directly shows the dynamic contribution that USP7 has upon RNF20 turnover, complementing the knockout and reconstitution assays conducted.

USP7 Deubiquitinates RNF20

To demonstrate that USP7 deubiquitinates RNF20, a deubiquitination assay was conducted (Figure 12). In this experiment, it was observed that under control conditions, RNF20 was heavily ubiquitinated. However, when wild-type USP7 (Myc-USP7) was co-transfected into the cells, there was a noticeable decrease in the ubiquitination levels of RNF20. Conversely, when the catalytically inactive C233S USP7 was co-transfected, it did not decrease the ubiquitination levels of RNF20 compared to wild-type USP7. This clear difference confirms that USP7 deubiquitinates RNF20 and that this process relies on USP7's catalytic activity. This assay provides direct evidence that RNF20 is a substrate of USP7 and indicates that the observed effects are not caused by secondary changes unrelated to deubiquitination. The clear difference in ubiquitination levels between wild-type USP7 and the catalytically inactive C233S mutant emphasizes the importance of the catalytic activity of USP7 for the active deubiquitination of RNF20, helping to maintain its stability.

Future Directions and Limitations

Although the interaction between USP7 and RNF20 was demonstrated, the domain-specific interaction at which RNF20 binds to USP7 was not determined. USP7 contains two different binding sites, one at the N-terminus, which recognizes the consensus sequence P/A/ExxS and another at the C-terminus UBL-domain, which recognizes the KxxxK motif on target substrates. Even though we have postulated that, due to RNF20 containing an ASSS motif,

the interaction will likely occur at the N-terminus ^{164}DWGF^{167} motif, in order to show this experimentally, a pulldown assay with wild-type and mutated N-terminus and C-terminus of USP7 or co-IP with various truncated USP7 constructs could be conducted. A further limitation is the absence of a siRNA-mediated USP7 knockdown assay to complement the knockout and overexpression experiments. This approach would provide an independent way of validating the USP7 and RNF20 relationship without requiring the use of the knockout USP7 cell line. Furthermore, USP7's role in stabilizing RNF20 abundance under cellular stress, such as DNA damage caused by UV exposure, can be analyzed, as RNF20 is involved in activating DNA damage response pathways through its interaction with histone H2B. The main downstream target of RNF20, which is histone H2B, is also regulated by USP7 directly, making it challenging to decipher if the changes in ubiquitination status on histone H2B observed by USP7 loss are due to the destabilization of RNF20, loss of USP7, or a combination of the two scenarios. Furthermore, many of the experiments were conducted with HCT116 cells alone and in future experiments, they should be done in various cell lines to confirm reproducibility and to confirm that the results are not cell/tissue specific.

Conclusion

In this thesis, we investigated the regulation of RNF20, an E3 ligase involved in histone H2B ubiquitination. The results identified USP7 as the deubiquitinating enzyme responsible for removing ubiquitin from RNF20 and stabilizing its protein levels, preventing its degradation by the proteasome. Using various biological techniques, including endogenous co-immunoprecipitation, comparisons between parental and USP7 knockout HCT116 cells,

reconstitution assays, overexpression of USP7 or its catalytic mutant, cycloheximide chase, and deubiquitination assays, we demonstrated that loss of USP7 increases RNF20 ubiquitination levels, leading to its degradation. Moreover, RNF20 stability depends not only on its interaction with USP7 but also on the catalytic activity of USP7. These findings open new research avenues to explore how USP7-RNF20 interactions regulate H2B ubiquitination and to develop potential therapeutic strategies targeting this pathway.

References

Blank, M., Tang, Y., Yamashita, M., Burkett, S. S., Cheng, S. Y., & Zhang, Y. E. (2012). A tumor suppressor function of Smurf2 associated with controlling chromatin landscape and genome stability through RNF20. *Nature Medicine*, *18*(2), 227–234. https://doi.org/10.1038/nm.2596

Buetow, L., & Huang, D. T. (2016). Structural insights into the catalysis and regulation of E3 ubiquitin ligases. *Nature Reviews Molecular Cell Biology*, *17*(10), 626–642. https://doi.org/10.1038/nrm.2016.91

Chavoshi, S., Egorova, O., Lacdao, I. K., Farhadi, S., Sheng, Y., & Saridakis, V. (2016). Identification of kaposi sarcoma herpesvirus (KSHV) vIRF1 protein as a novel interaction partner of human deubiquitinase USP7. *Journal of Biological Chemistry*, *291*(12), 6281–6291. https://doi.org/10.1074/jbc.M115.710632

Cotton, T. R., & Lechtenberg, B. C. (2020). Chain reactions: molecular mechanisms of RBR ubiquitin ligases. *Biochemical Society Transactions*, *48*(4), 1737–1750. https://doi.org/10.1042/BST20200237

Dar, A., Shibata, E., & Dutta, A. (2013). Deubiquitination of Tip60 by USP7 Determines the Activity of the p53-Dependent Apoptotic Pathway. *Molecular and Cellular Biology*, *33*(16), 3309. https://doi.org/10.1128/MCB.00358-13

Du, Z., Song, J., Wang, Y., Zhao, Y., Guda, K., Yang, S., Kao, H. Y., Xu, Y., Willis, J., Markowitz, S. D., Sedwick, D., Ewing, R. M., & Wang, Z. (2010). DNMT1 Stability Is Regulated by Proteins Coordinating Deubiquitination and Acetylation-Driven Ubiquitination. *Science Signaling*, *3*(146), ra80. https://doi.org/10.1126/SCISIGNAL.2001462

Duan, Y., Huo, D., Gao, J., Wu, H., Ye, Z., Liu, Z., Zhang, K., Shan, L., Zhou, X., Wang, Y., Su, D., Ding, X., Shi, L., Wang, Y., Shang, Y., & Xuan, C. (2016). Ubiquitin ligase RNF20/40 facilitates spindle assembly and promotes breast carcinogenesis through stabilizing motor protein Eg5. *Nature Communications*, *7*(1), 12648. https://doi.org/10.1038/ncomms12648

Faesen, A. C., Dirac, A. M. G., Shanmugham, A., Ovaa, H., Perrakis, A., & Sixma, T. K. (2011). Mechanism of USP7/HAUSP activation by its C-Terminal ubiquitin-like domain and allosteric regulation by GMP-synthetase. *Molecular Cell*, *44*(1), 147–159. https://doi.org/10.1016/j.molcel.2011.06.034

Felle, M., Joppien, S., Németh, A., Diermeier, S., Thalhammer, V., Dobner, T., Kremmer, E., Kappler, R., & Längst, G. (2011). The USP7/Dnmt1 complex stimulates the DNA methylation

activity of Dnmt1 and regulates the stability of UHRF1. *Nucleic Acids Research*, *39*(19), 8355. https://doi.org/10.1093/NAR/GKR528

Foglizzo, M., Middleton, A. J., & Day, C. L. (2016). Structure and Function of the RING Domains of RNF20 and RNF40, Dimeric E3 Ligases that Monoubiquitylate Histone H2B. *Journal of Molecular Biology*, *428*(20), 4073–4086. https://doi.org/10.1016/j.jmb.2016.07.025

Gagarina, V., Bojagora, A., Lacdao, I. K., Luthra, N., Pfoh, R., Mohseni, S., Chaharlangi, D., Tan, N., & Saridakis, V. (2020). Structural Basis of the Interaction Between Ubiquitin Specific Protease 7 and Enhancer of Zeste Homolog 2. *Journal of Molecular Biology*, *432*(4), 897–912. https://doi.org/10.1016/J.JMB.2019.12.026

Haglund, K., Sigismund, S., Polo, S., Szymkiewicz, I., Di Fiore, P. P., & Dikic, I. (2003). Multiple monoubiquitination of RTKs is sufficient for their endocytosis and degradation. *Nature Cell Biology*, *5*(5), 461–466. https://doi.org/10.1038/ncb983

Hahn, M. A., Dickson, K.-A., Jackson, S., Clarkson, A., Gill, A. J., & Marsh, D. J. (2012). The tumor suppressor CDC73 interacts with the ring finger proteins RNF20 and RNF40 and is required for the maintenance of histone 2B monoubiquitination. *Human Molecular Genetics*, *21*(3), 559–568. https://doi.org/10.1093/hmg/ddr490

Heride, C., Urbé, S., & Clague, M. J. (2014). Ubiquitin code assembly and disassembly. *Current Biology*, *24*(6), R215–R220. https://doi.org/10.1016/j.cub.2014.02.002

Holowaty, M. N., Zeghouf, M., Wu, H., Tellam, J., Athanasopoulos, V., Greenblatt, J., & Frappier, L. (2003). Protein profiling with Epstein-Barr nuclear antigen-1 reveals an interaction with the herpesvirus-associated ubiquitin-specific protease HAUSP/USP7. *Journal of Biological Chemistry*, *278*(32), 29987–29994. https://doi.org/10.1074/JBC.M303977200/ASSET/6EF64E36-50D1-445D-8E68-996B60557AC7/MAIN.ASSETS/GR7.JPG

Hu, M., Li, P., Li, M., Li, W., Yao, T., Wu, J. W., Gu, W., Cohen, R. E., & Shi, Y. (2002). Crystal structure of a UBP-family deubiquitinating enzyme in isolation and in complex with ubiquitin aldehyde. *Cell*, *111*(7), 1041–1054. https://doi.org/10.1016/S0092-8674(02)01199-6

Ji, L., Lu, B., Zamponi, R., Charlat, O., Aversa, R., Yang, Z., Sigoillot, F., Zhu, X., Hu, T., Reece-Hoyes, J. S., Russ, C., Michaud, G., Tchorz, J. S., Jiang, X., & Cong, F. (2019). USP7 inhibits Wnt/β-catenin signaling through promoting stabilization of Axin. *Nature Communications*, *10*(1), 1–14. https://doi.org/10.1038/S41467-019-12143-3;TECHMETA

Jiang, L., Xiong, J., Zhan, J., Yuan, F., Tang, M., Zhang, C., Cao, Z., Chen, Y., Lu, X., Li, Y., Wang, H., Wang, L., Wang, J., Zhu, W. G., & Wang, H. (2017). Ubiquitin-specific peptidase 7 (USP7)-

mediated deubiquitination of the histone deacetylase SIRT7 regulates gluconeogenesis. *The Journal of Biological Chemistry*, *292*(32), 13296. https://doi.org/10.1074/JBC.M117.780130

Jin, Q., Martinez, C. A., Arcipowski, K. M., Zhu, Y., Gutierrez-Diaz, B. T., Wang, K. K., Johnson, M. R., Volk, A. G., Wang, F., Wu, J., Grove, C., Wang, H., Sokirniy, I., Thomas, P. M., Goo, Y. A., Abshiru, N. A., Hijiya, N., Peirs, S., Vandamme, N., … Ntziachristos, P. (2018). USP7 cooperates with NOTCH1 to drive the oncogenic transcriptional program in T cell leukemia. *Clinical Cancer Research : An Official Journal of the American Association for Cancer Research*, *25*(1), 222. https://doi.org/10.1158/1078-0432.CCR-18-1740

Jumper, J., Evans, R., Pritzel, A., Green, T., Figurnov, M., Ronneberger, O., Tunyasuvunakool, K., Bates, R., Žídek, A., Potapenko, A., Bridgland, A., Meyer, C., Kohl, S. A. A., Ballard, A. J., Cowie, A., Romera-Paredes, B., Nikolov, S., Jain, R., Adler, J., … Hassabis, D. (2021). Highly accurate protein structure prediction with AlphaFold. *Nature*, *596*(7873), 583–589. https://doi.org/10.1038/s41586-021-03819-2

Keijzer, N., Priyanka, A., Stijf-Bultsma, Y., Fish, A., Gersch, M., & Sixma, T. K. (2024). Variety in the USP deubiquitinase catalytic mechanism. *Life Science Alliance*, *7*(4), e202302533. https://doi.org/10.26508/lsa.202302533

Kim, R. Q., van Dijk, W. J., & Sixma, T. K. (2016). Structure of USP7 catalytic domain and three Ubl-domains reveals a connector α-helix with regulatory role. *Journal of Structural Biology*, *195*(1), 11–18. https://doi.org/10.1016/J.JSB.2016.05.005

Komander, D., Clague, M. J., & Urbé, S. (2009). Breaking the chains: structure and function of the deubiquitinases. *Nature Reviews Molecular Cell Biology*, *10*(8), 550–563. https://doi.org/10.1038/nrm2731

Ku, M., Koche, R. P., Rheinbay, E., Mendenhall, E. M., Endoh, M., Mikkelsen, T. S., Presser, A., Nusbaum, C., Xie, X., Chi, A. S., Adli, M., Kasif, S., Ptaszek, L. M., Cowan, C. A., Lander, E. S., Koseki, H., & Bernstein, B. E. (2008). Genomewide Analysis of PRC1 and PRC2 Occupancy Identifies Two Classes of Bivalent Domains. *PLoS Genetics*, *4*(10), e1000242. https://doi.org/10.1371/JOURNAL.PGEN.1000242

Kwon, Y., Vinayagam, A., Sun, X., Dephoure, N., Gygi, S. P., Hong, P., & Perrimon, N. (2013). The Hippo Signaling Pathway Interactome. *Science (New York, N.Y.)*, *342*(6159), 737. https://doi.org/10.1126/SCIENCE.1243971

Li, Y., & Reverter, D. (2021). Molecular Mechanisms of DUBs Regulation in Signaling and Disease. *International Journal of Molecular Sciences*, *22*(3), 986. https://doi.org/10.3390/ijms22030986

Liu, J., Cheng, Y., Zheng, M., Yuan, B., Wang, Z., Li, X., Yin, J., Ye, M., & Song, Y. (2021). Targeting the ubiquitination/deubiquitination process to regulate immune checkpoint pathways. *Signal Transduction and Targeted Therapy*, *6*(1), 28. https://doi.org/10.1038/s41392-020-00418-x

Liu, X., & Liu, X. (2022). PRC2, Chromatin Regulation, and Human Disease: Insights From Molecular Structure and Function. *Frontiers in Oncology*, *12*, 894585. https://doi.org/10.3389/FONC.2022.894585

Lyu, Y., Yang, Y., Talwar, V., Lu, H., Chen, C., Salman, S., Wicks, E. E., Huang, T. Y.-T., Drehmer, D., Wang, Y., Zuo, Q., Datan, E., Jackson, W., Dordai, D., Wang, R., & Semenza, G. L. (2024). Hypoxia-inducible factor 1 recruits FACT and RNF20/40 to mediate histone ubiquitination and transcriptional activation of target genes. *Cell Reports*, *43*(4), 113972. https://doi.org/10.1016/j.celrep.2024.113972

Mao, Y. (2021). Structure, Dynamics and Function of the 26S Proteasome. *Subcellular Biochemistry*, *96*, 1–151. https://doi.org/10.1007/978-3-030-58971-4_1/FIGURES/2

Mevissen, T. E. T., Hospenthal, M. K., Geurink, P. P., Elliott, P. R., Akutsu, M., Arnaudo, N., Ekkebus, R., Kulathu, Y., Wauer, T., El Oualid, F., Freund, S. M. V., Ovaa, H., & Komander, D. (2013). OTU Deubiquitinases Reveal Mechanisms of Linkage Specificity and Enable Ubiquitin Chain Restriction Analysis. *Cell*, *154*(1), 169–184. https://doi.org/10.1016/j.cell.2013.05.046

Musaus, M., Navabpour, S., & Jarome, T. J. (2020). The diversity of linkage-specific polyubiquitin chains and their role in synaptic plasticity and memory formation. *Neurobiology of Learning and Memory*, *174*, 107286. https://doi.org/10.1016/j.nlm.2020.107286

Onishi, S., Uchiyama, K., Sato, K., Okada, C., Kobayashi, S., Hamada, K., Nishizawa, T., Nureki, O., Ogata, K., & Sengoku, T. (2024). Structure of the human Bre1 complex bound to the nucleosome. *Nature Communications*, *15*(1), 2580. https://doi.org/10.1038/S41467-024-46910-8

Pan, X., Wu, S., Wei, W., Chen, Z., Wu, Y., & Gong, K. (2022). Structural and Functional Basis of JAMM Deubiquitinating Enzymes in Disease. *Biomolecules*, *12*(7), 910. https://doi.org/10.3390/biom12070910

Pfoh, R., Lacdao, I. K., Georges, A. A., Capar, A., Zheng, H., Frappier, L., & Saridakis, V. (2015). Crystal Structure of USP7 Ubiquitin-like Domains with an ICP0 Peptide Reveals a Novel Mechanism Used by Viral and Cellular Proteins to Target USP7. *PLoS Pathogens*, *11*(6), e1004950. https://doi.org/10.1371/JOURNAL.PPAT.1004950

Pickart, C. M., & Eddins, M. J. (2004). Ubiquitin: structures, functions, mechanisms. *Biochimica et Biophysica Acta (BBA) - Molecular Cell Research*, *1695*(1–3), 55–72. https://doi.org/10.1016/j.bbamcr.2004.09.019

Pozhidaeva, A., & Bezsonova, I. (2019). USP7: structure, substrate specificity, and inhibition. *DNA Repair*, *76*, 30. https://doi.org/10.1016/J.DNAREP.2019.02.005

Rougé, L., Bainbridge, T. W., Kwok, M., Tong, R., Di Lello, P., Wertz, I. E., Maurer, T., Ernst, J. A., & Murray, J. (2016). Molecular Understanding of USP7 Substrate Recognition and C-Terminal Activation. *Structure*, *24*(8), 1335–1345. https://doi.org/10.1016/j.str.2016.05.020

Saridakis, V., Sheng, Y., Sarkari, F., Holowaty, M. N., Shire, K., Nguyen, T., Zhang, R. G., Liao, J., Lee, W., Edwards, A. M., Arrowsmith, C. H., & Frappier, L. (2005). Structure of the p53 binding domain of HAUSP/USP7 bound to epstein-barr nuclear antigen 1: Implications for EBV-mediated immortalization. *Molecular Cell*, *18*(1), 25–36. https://doi.org/10.1016/j.molcel.2005.02.029

Sethi, G., Shanmugam, M. K., Arfuso, F., & Kumar, A. P. (2018). Role of RNF20 in cancer development and progression – a comprehensive review. *Bioscience Reports*, *38*(4). https://doi.org/10.1042/BSR20171287

Sheng, Y., Saridakis, V., Sarkari, F., Duan, S., Wu, T., Arrowsmith, C. H., & Frappier, L. (2006). Molecular recognition of p53 and MDM2 by USP7/HAUSP. *Nature Structural and Molecular Biology*, *13*(3), 285–291. https://doi.org/10.1038/NSMB1067;KWRD=LIFE+SCIENCES

Shiloh, Y., Shema, E., Moyal, L., & Oren, M. (2011). RNF20–RNF40: A ubiquitin-driven link between gene expression and the DNA damage response. *FEBS Letters*, *585*(18), 2795–2802. https://doi.org/10.1016/j.febslet.2011.07.034

Sowa, M. E., Bennett, E. J., Gygi, S. P., & Harper, J. W. (2009). Defining the Human Deubiquitinating Enzyme Interaction Landscape. *Cell*, *138*(2), 389–403. https://doi.org/10.1016/j.cell.2009.04.042

Su, D., Wang, W., Hou, Y., Wang, L., Yi, X., Cao, C., Wang, Y., Gao, H., Wang, Y., Yang, C., Liu, B., Chen, X., Wu, X., Wu, J., Yan, D., Wei, S., Han, L., Liu, S., Wang, Q., … Shan, L. (2021). Bimodal regulation of the PRC2 complex by USP7 underlies tumorigenesis. *Nucleic Acids Research*, *49*(8), 4421. https://doi.org/10.1093/NAR/GKAB209

Varadi, M., Anyango, S., Deshpande, M., Nair, S., Natassia, C., Yordanova, G., Yuan, D., Stroe, O., Wood, G., Laydon, A., Žídek, A., Green, T., Tunyasuvunakool, K., Petersen, S., Jumper, J., Clancy, E., Green, R., Vora, A., Lutfi, M., … Velankar, S. (2022). AlphaFold Protein Structure Database: massively expanding the structural coverage of protein-sequence space with

high-accuracy models. *Nucleic Acids Research*, *50*(D1), D439–D444. https://doi.org/10.1093/nar/gkab1061

Wang, D., Wang, Y., Wu, X., Kong, X., Li, J., & Dong, C. (2020). RNF20 Is Critical for Snail-Mediated E-Cadherin Repression in Human Breast Cancer. *Frontiers in Oncology*, *10*. https://doi.org/10.3389/fonc.2020.613470

Wang, Z., Kang, W., You, Y., Pang, J., Ren, H., Suo, Z., Liu, H., & Zheng, Y. (2019). USP7: Novel Drug Target in Cancer Therapy. *Frontiers in Pharmacology*, *10*(APR), 427. https://doi.org/10.3389/FPHAR.2019.00427

Weissman, A. M. (2001). Themes and variations on ubiquitylation. *Nature Reviews Molecular Cell Biology*, *2*(3), 169–178. https://doi.org/10.1038/35056563

Wojcik, F., Dann, G. P., Beh, L. Y., Debelouchina, G. T., Hofmann, R., & Muir, T. W. (2018). Functional crosstalk between histone H2B ubiquitylation and H2A modifications and variants. *Nature Communications*, *9*(1), 1394. https://doi.org/10.1038/s41467-018-03895-5

Wolberger, C. (2014). Mechanisms for regulating deubiquitinating enzymes. *Protein Science*, *23*(4), 344–353. https://doi.org/10.1002/pro.2415

Xu, Z. (2024). Potential roles of UCH family deubiquitinases in tumorigenesis and chemical inhibitors developed against them. *American Journal of Cancer Research*, *14*(6), 2666–2694. https://doi.org/10.62347/OEGE2648

Yang, J.-M., Schiapparelli, P., Nguyen, H.-N., Igarashi, A., Zhang, Q., Abbadi, S., Amzel, L. M., Sesaki, H., Quiñones-Hinojosa, A., & Iijima, M. (2017). Characterization of PTEN mutations in brain cancer reveals that pten mono-ubiquitination promotes protein stability and nuclear localization. *Oncogene*, *36*(26), 3673–3685. https://doi.org/10.1038/onc.2016.493

Yim, H., Shin, S. B., Woo, S. U., Lee, P. C. W., & Erikson, R. L. (2017). Plk1-mediated stabilization of 53BP1 through USP7 regulates centrosome positioning to maintain bipolarity. *Oncogene*, *36*(7), 966–978. https://doi.org/10.1038/ONC.2016.263;TECHMETA

Zhou, B., Lin, W., Long, Y., Yang, Y., Zhang, H., Wu, K., & Chu, Q. (2022). Notch signaling pathway: architecture, disease, and therapeutics. *Signal Transduction and Targeted Therapy*, *7*(1), 1–33. https://doi.org/10.1038/S41392-022-00934-Y;SUBJMETA

Zhou, L., Ouyang, T., Li, M., Hong, T., MHS, A., Meng, W., & Zhang, N. (2021). Ubiquitin-Specific Peptidase 7: A Novel Deubiquitinase That Regulates Protein Homeostasis and Cancers. *Frontiers in Oncology*, *11*. https://doi.org/10.3389/fonc.2021.784672

Ziv, I., Matiuhin, Y., Kirkpatrick, D. S., Erpapazoglou, Z., Leon, S., Pantazopoulou, M., Kim, W., Gygi, S. P., Haguenauer-Tsapis, R., Reis, N., Glickman, M. H., & Kleifeld, O. (2011). A Perturbed Ubiquitin Landscape Distinguishes Between Ubiquitin in Trafficking and in Proteolysis. *Molecular & Cellular Proteomics*, *10*(5), M111.009753. https://doi.org/10.1074/mcp.M111.009753

Zlatanou, A., Sabbioneda, S., Miller, E. S., Greenwalt, A., Aggathanggelou, A., Maurice, M. M., Lehmann, A. R., Stankovic, T., Reverdy, C., Colland, F., Vaziri, C., & Stewart, G. S. (2016). USP7 is essential for maintaining Rad18 stability and DNA damage tolerance. *Oncogene*, *35*(8), 965–976. https://doi.org/10.1038/ONC.2015.149;TECHMETA